Marine and Petroleum Geology 117 (2020) 104392

Contents lists available at ScienceDirect

Marine and Petroleum Geology

journal homepage: www.elsevier.com/locate/marpetgeo

Research paper

Contourite porosity, grain size and reservoir characteristics

Xiaohang Yu[a], Dorrik Stow[b,a,*], Zeinab Smillie[b], Ibimina Esentia[b], Rachel Brackenridge[b,1], Xinong Xie[a], Shereef Bankole[b], Emmanuelle Ducassou[c], Estefania Llave[d]

[a] College of Marine Science and Technology, China University of Geosciences, Wuhan, China
[b] Institute of Geo-Energy Engineering, School of Energy, Geoscience, Infrastructure & Society, Heriot-Watt University, Edinburgh, EH14 4AS, UK
[c] Department of Oceanography, Bordeaux University, Bordeaux, France
[d] Instituto Geológico y Minero de España, Rios Rosas 23, 28003, Madrid, Spain

ARTICLE INFO

Keywords:
Contourites
Porosity-depth trends
Grain size characteristics
Reservoir characteristics

ABSTRACT

Contourites are now recognised as having a significant potential as hydrocarbon reservoirs in the subsurface, and several fields have been interpreted as comprising bottom-current reworked turbidite sands. However, very little has been published on the porosity characteristics of contourites. This study documents porosity data from IODP Expedition 339 sites in the Gulf of Cadiz. We use grain size analyses, porosity-depth plots and exponential models to yield a better understanding of grain size characteristics and facies, porosity characteristics, and the reservoir potential of contourites in the subsurface.

New grain size data for over 350 samples from the Cadiz contourites is presented, building on earlier work. These data confirm the distinctive trends in textural properties linked to depositional processes under the action of bottom currents. The finest muddy contourites (< 20 μm) show normal grain size distributions, poor to very poor sorting becoming better with decreasing grain size, and zero or low skewness. These are contourite-hemipelagite hybrids. Muddy to fine sandy contourites (20–200 μm) trend towards better sorting and initially fine-tail and then coarse-tail skew. These represent typical depositional trends for contourites, affected by current capacity and then increased winnowing at higher current speed. Clean sandy contourites (around 200 μm) are the best sorted. Medium and coarser-grained contourites show a trend towards poorer sorting. They result from the action of dominant bedload transport, extensive winnowing, and mixed sediment supply.

Porosity-depth relationships from four Cadiz sites show a moderately high initial porosity for both sand and mud facies (50–60%) and a systematic decrease with depth to around 35–40% near 500 m burial depth. According to the exponential models of porosity with depth, contourite porosity should exceed 10% at 2500 m burial depth. We compare the data from the Gulf of Cadiz Contourite Depositional System, with those of the Eirik Drift, Newfoundland Drift, Gardar Drift and Canterbury Slope Drifts. Similar depth trends are observed, and all show anomalies linked to interbedded sandy and muddy facies, composition (carbonate vs siliciclastic), and the presence of hiatuses in the sediment record.

These data provide good insight into the likely reservoir characteristics of contourites, for both conventional and unconventional reservoirs. They are comparable with those of existing contourite fields, most of which are mixed turbidite-contourite systems.

1. Introduction

Contourites are deep-water sediments deposited or substantially reworked by bottom currents. They are commonly interbedded with other deep-water facies due to the interaction of different kinds of currents (Rebesco and Camerlenghi, 2008). Since Hollister and Heezen (1972) first defined the concept of contourites, the understanding of these sediments has increased considerably, mainly focused on sedimentary characteristics, facies models, and controlling factors (Faugères and Stow, 1993; Viana et al., 1998; Stow and Mayall, 2000; Stow et al., 2002b; Rebesco and Camerlenghi, 2008; Stow and Faugères, 2008; Rebesco et al., 2014). Contourite drifts are widely distributed around the world (Rebesco and Camerlenghi, 2008; Chen et al., 2014; Rebesco et al., 2014; Wen et al., 2016), and are recognised as providing significant opportunity for future

* Corresponding author. Institute of Geo-Energy Engineering, School of Energy, Geoscience, Infrastructure & Society, Heriot-Watt University, Edinburgh, EH14 4AS, UK.
E-mail address: d.stow@hw.ac.uk (D. Stow).
[1] Now, School of Geosciences, University of Aberdeen, Kings College, Aberdeen AB24 3FX.

https://doi.org/10.1016/j.marpetgeo.2020.104392
Received 14 January 2020; Received in revised form 2 April 2020; Accepted 7 April 2020
Available online 12 April 2020
0264-8172/

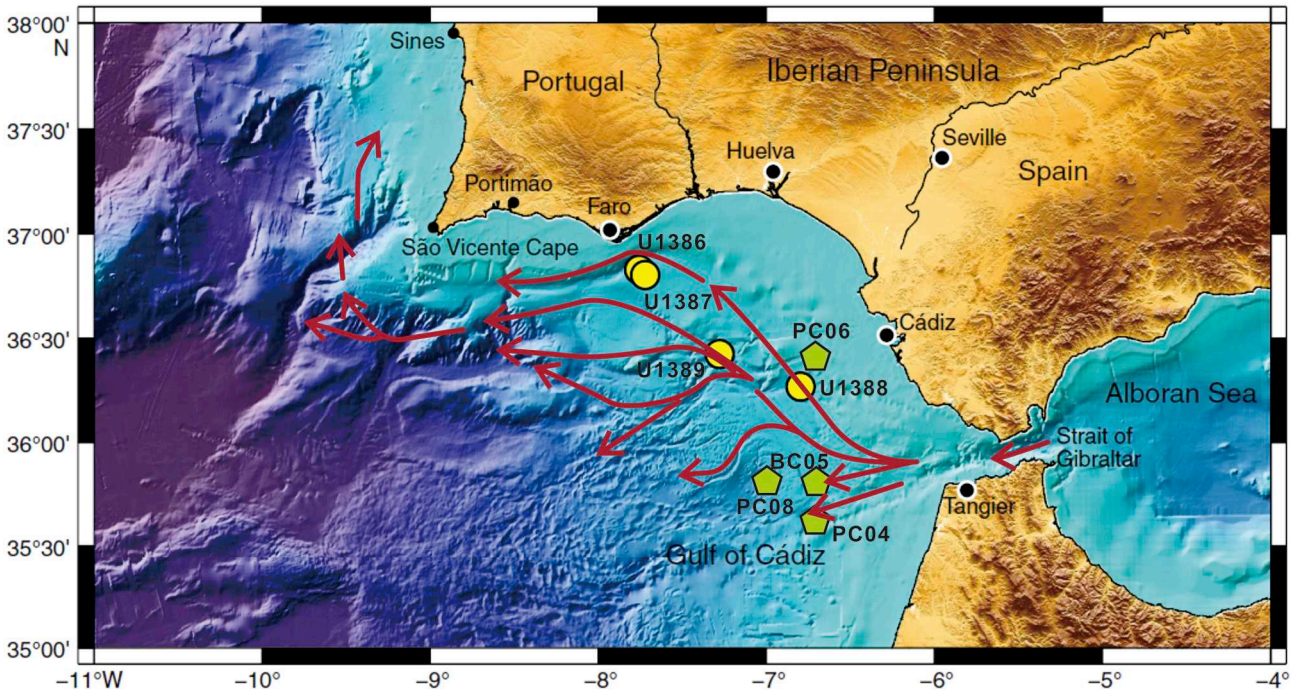

Fig. 1. Morphological map of the Gulf of Cadiz. The yellow circles show the locations of the sites U1386, U1387, U1388 and U1389 of IODP 339, and the green pentagons show the locations of BC04, PC04, PC06 and PC08 of the CONTOURIBER-1 expedition. The red lines mark the principal bottom-currents associated with the Mediterranean Outflow Water. Modified from Hernández-Molina et al. (2006) and Expedition 339 Scientists (2013). (For interpretation of the references to colour in this figure legend, the reader is referred to the Web version of this article.)

petroleum exploration (Stow and Mayall, 2000; Pettingill and Weimer, 2002; Viana et al., 2007; Shanmugam, 2012). Recent research on sandy contourite systems, such as the Cadiz sand sheet (Stow et al., 2013b), Falkland sand sheet (Nicholson and Stow, 2019), Faroe–Shetland Channel (Masson et al., 2010), and Riffian Corridor contourite sands (Capella et al., 2017), combined with better understanding of unconventional reservoirs, have re-invigorated research into the economic value of contourites. However, much work is still needed to better characterise contourites as potential reservoirs, including their texture, porosity and permeability attributes (Viana et al., 2007; Brackenridge et al., 2018).

This paper focuses in particular on the grain size and porosity of contourites, presenting new data from the Gulf of Cadiz contourite depositional system, offshore Spain, derived from four sites (U1386, U1387, U1388 and U1389) of the Integrated Ocean Drilling Program (IODP) Expedition 339. These are combined with grain-size data from CONTOURIBER sites (BC05, PC04, PC06 and PC08) as published by Brackenridge et al. (2018) (Fig. 1). We also access porosity data from four other IODP sites for comparison, on Newfoundland drift, Eirik drift, Gardar drift and Canterbury slope. In summary, the aims of this paper are as follows:

1) To discuss new grain size data from Cadiz contourites and so develop our understanding of contourite depositional processes and their potential as hydrocarbon reservoirs.
2) To present porosity-depth relationships for both the Cadiz contourites and comparative drift systems, and to use exponential models for evaluating the potential porosities at reservoir depths.
3) To consider these data in terms of the reservoir characteristics of contourites.

2. Methods and database

2.1. Site data

The large Contourite Depositional System (CDS) of Gulf of Cadiz was deposited under the influence of warm, high-salinity Mediterranean Outflow Water from Pliocene to Recent (Fig. 1). It is now well established as one of the prime contourite depositional laboratories in the world (Maldonado et al., 1999; Stow et al., 2013b; Hernández-Molina et al., 2016a).

Five sites were drilled during IODP Expedition 339 in the Gulf of Cadiz CDS, at between 570 and 1100 m water depths. These recovered a total of 4.5 km of core material using the advanced piston corer system, the extended core barrel system, and the rotary core barrel system (Stow et al., 2013a, 2014). This study mainly focuses on geological data and core data (sediments and physical properties) from four of these sites: U1386, U1387, U1388 and U1389. We further present porosity-depth data derived from four other expeditions that drilled contourite systems, namely IODP 303 site 1305, IODP 317 site 1352, IODP 342 site U1410, and IODP 303 site 1304 (Channell et al., 2006; Fulthorpe et al., 2011; Norris et al., 2014). This database is summarised in Table 1.

2.2. Facies and porosity data

Sediment facies and their interpretation are well known for the Cadiz sites, as they have been extensively studied by several of the present authors (Stow et al., 2013b; Hernandez-Molina et al., 2014; Alonso et al., 2016; Hernández-Molina et al., 2016a; Brackenridge et al., 2018). One of us (Dorrik Stow) has further examined cores from each of the other four sites used in this study, and concurs with shipboard scientists in their interpretation of mainly contourite, pelagite and hemipelagite sedimentation.

Porosity data was measured by determination of moisture and density method (Stow et al., 2013a) on discrete sediment samples. The working halves divided from whole-round cores were used for taking discrete samples to determine the porosity. About 10 cm^3 samples from soft sediments were collected by a plastic syringe and sampled every other section per core at the 59–60 cm position. Dry sample volume was measured by a hexapycnometer system of a six-celled, custom-configured Micromeritics AccuPyc 1330 TC helium-displacement

Table 1
Data summary of site U1386, site U1387, site U1388, site U1389 of IODP 339, site U1305 of IODP 303, site U1304 of IODP 303site, U1352 of IODP 317 and site U13410 of IODP 342 (Channell et al., 2006; Fulthorpe et al., 2011; Stow et al., 2013a; Norris et al., 2014).

Expedition	Site	Number of holes	Distance between adjacent holes (m)	Lat/long	Water depth (m)	Drift name	Total core recovery (m)	Porosity sample amount
IODP 339	U1386	3	20	36°49.685′N; 7°45.321′W	561	CDS of Gulf of Cadiz	850.64	197
IODP 339	U1387	3	20	36°48.3210′; 7°43.1321′W	559	CDS of Gulf of Cadiz	1084.95	213
IODP 339	U1388	3	20	36°16.142′N; 6°47.648′W	663	CDS of Gulf of Cadiz	121	47
IODP 339	U1389	5	20	36°25.515′N; 7°16.683′W	644	CDS of Gulf of Cadiz	1123.5	200
IODP 303	U1305	3	20	57°28.5066′; 48°31.8132′W	3459	Eirik Drift	867.13	31
IODP 303	U1304	4	20	53°3.4007′N; 33°31.7814′W	3024	Gardar Drift	251.37	50
IODP 342	U1410	3	20	41°19.6993′N; 49°10.1847′W	3387	Newfoundland Drift	748.8	143
IODP 317	U1352	4	20	44°56.2440′S; 172°1.3615′E	344	Canterbury Slope Drift	1443.65	1268

pycnometer. The measurement focuses on the principal lithology of a section, and avoids small intelayers of different grain size. Porosity (ϕ) data is calculated as $\phi = V_{pw}/V_{wet}$. The determination procedures of these physical properties refer to the American Society for Testing and Materials (ASTM) designation (D) 2216 (ASTM International, 1990). The porosity data used in this study from each of the four other IODP sites was also measured and calculated by the discrete moisture and density measurement technique (Channell et al., 2006; Fulthorpe et al., 2011; Norris et al., 2014).

2.3. Grain size analysis

For this study, a total of 350 samples were analysed for grain size at the University of Bordeaux, with a Malvern Laser Particle Size Analyser, following the procedures used by Brackenridge et al. (2018) in their recent exposition of contourite textural characteristics. This measured grain sizes from 0.05 μm to 700 μm. The standard procedure for grain size analysis in laser counters was used (McCave et al., 1986; Cooper, 1998; Martins, 2003). Distributions are given in a geometric (volume) scaling rather than arithmetic (number) scale to ensure there is equal emphasis on changes in clay, silt and sand content in the histogram (Blott and Pye, 2001). All analysis was carried out in the software GRADISTAT (Blott and Pye, 2001) using the geometric graphical method as laid out by Folk and Ward (1957) to ensure that each set of analysis can be directly compared to others in the study. Key statistical measures include: mean, sorting (standard deviation), skewness, and kurtosis. The formulae used for these measurements and the cut-off values for defining the sorting, skewness and kurtosis are outlined in Blott and Pye (2001). After calculation of the essential statistics, data were compared using cross plots (Folk and Robles, 1964; Martins, 2003); the sediment classes are as defined by Wentworth (1922).

3. Results

3.1. Sediment facies and distribution: Gulf of Cadiz

The principal sediment facies recovered from the IODP drilling (Stow et al., 2013a) throughout the six sites on the Cadiz Contourite Depositional System include muds, silts and muddy sands. These are primarily siliciclastic in composition with a minor to common (5–30%) calcareous biogenic fraction. Minor facies include: muddy calcareous sediments (> 50% $CaCO_3$) and foram-nannofossil ooze, which occur solely within the Miocene succession at Sites U1386 and U1387; dolomitic mudstone and dolostone, which occur locally at two sites (U1387 and U1391) within the early Pliocene; and clean sandstone beds and chaotic clast-rich units, within the early Quaternary and Pliocene at Sites U1386 and U1387.

These facies have been well documented in previous publications (e.g. Hernández-Molina et al., 2016a) and have been interpreted in terms of depositional processes as contourites, turbidites, reworked turbidites, debrites and slump deposits, pelagites and hemipelagites (Stow et al., 2013b; Alonso et al., 2016; Hernández-Molina et al., 2016a) (Figs. 2 and 3). We are very confident of these interpretations, which are based on multiple criteria at different scales of observation: small-scale sedimentary characteristics (structures, textures, composition, fabric), medium-scale seismic features (drifts, moats, seismic facies, widespread hiatuses), and the large-scale geological and oceanographic setting.

Contourites are the dominant sediment type at the six CDS sites (U1386-U1391), making up 95% of the Quaternary and about 50% of the recovered Pliocene succession. This facies group includes sand-rich, muddy sand, silty-mud and mud-rich contourites, all of which were deposited at moderate (20–30 cm/ka to very high (> 100 cm/ka) rates of sedimentation. Clean, well-cemented sands are common in the lowermost 20–40 m of the Quaternary succession at site U1386 and also present in the same stratigraphic interval at site U1387. These are

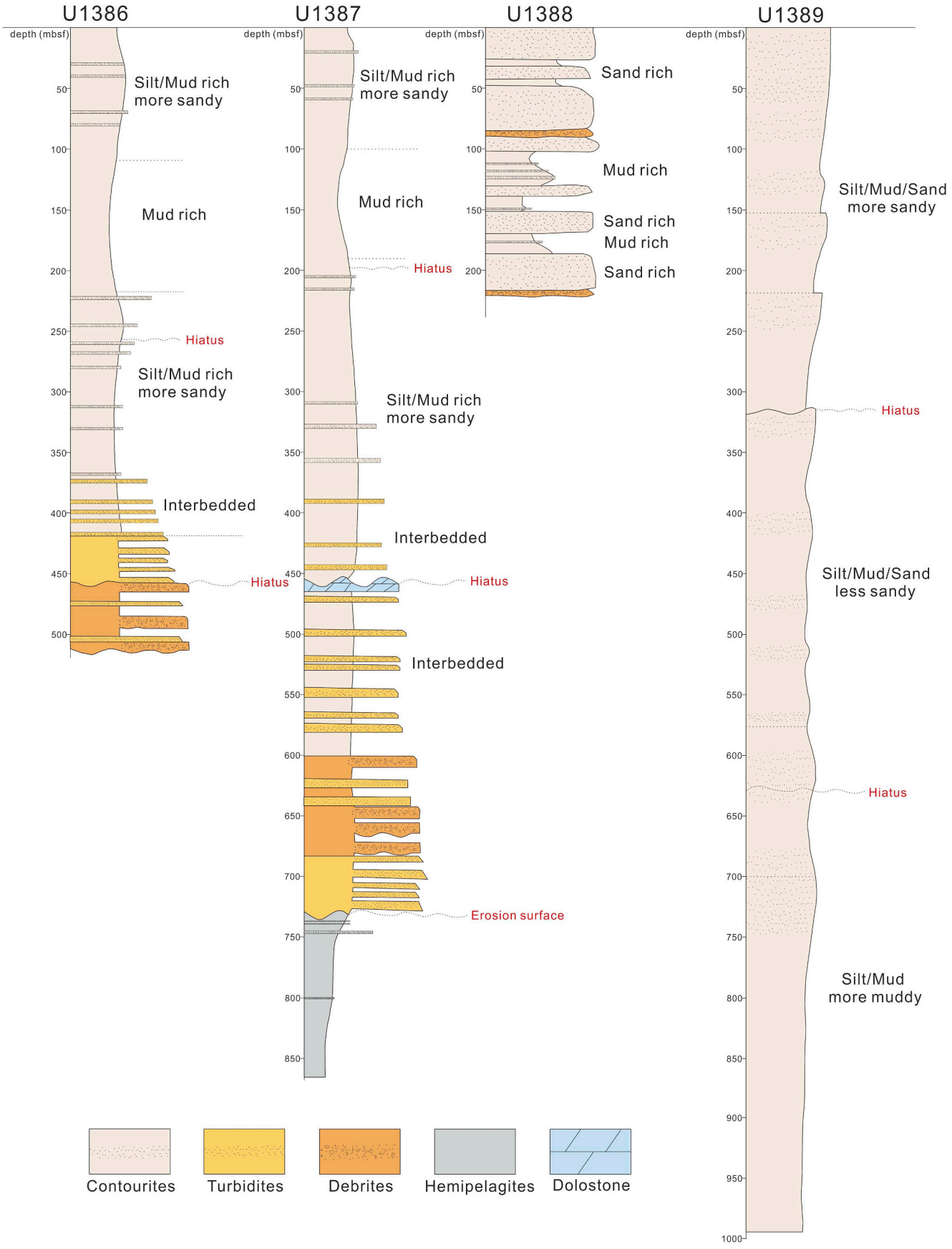

Fig. 2. Summary well logs for IODP 339 sites U1386, U1387, U1388 and U1389 in the Gulf of Cadiz, with schematic representation of the main facies present, and principal hiatuses. mbsf = metres below sea floor.

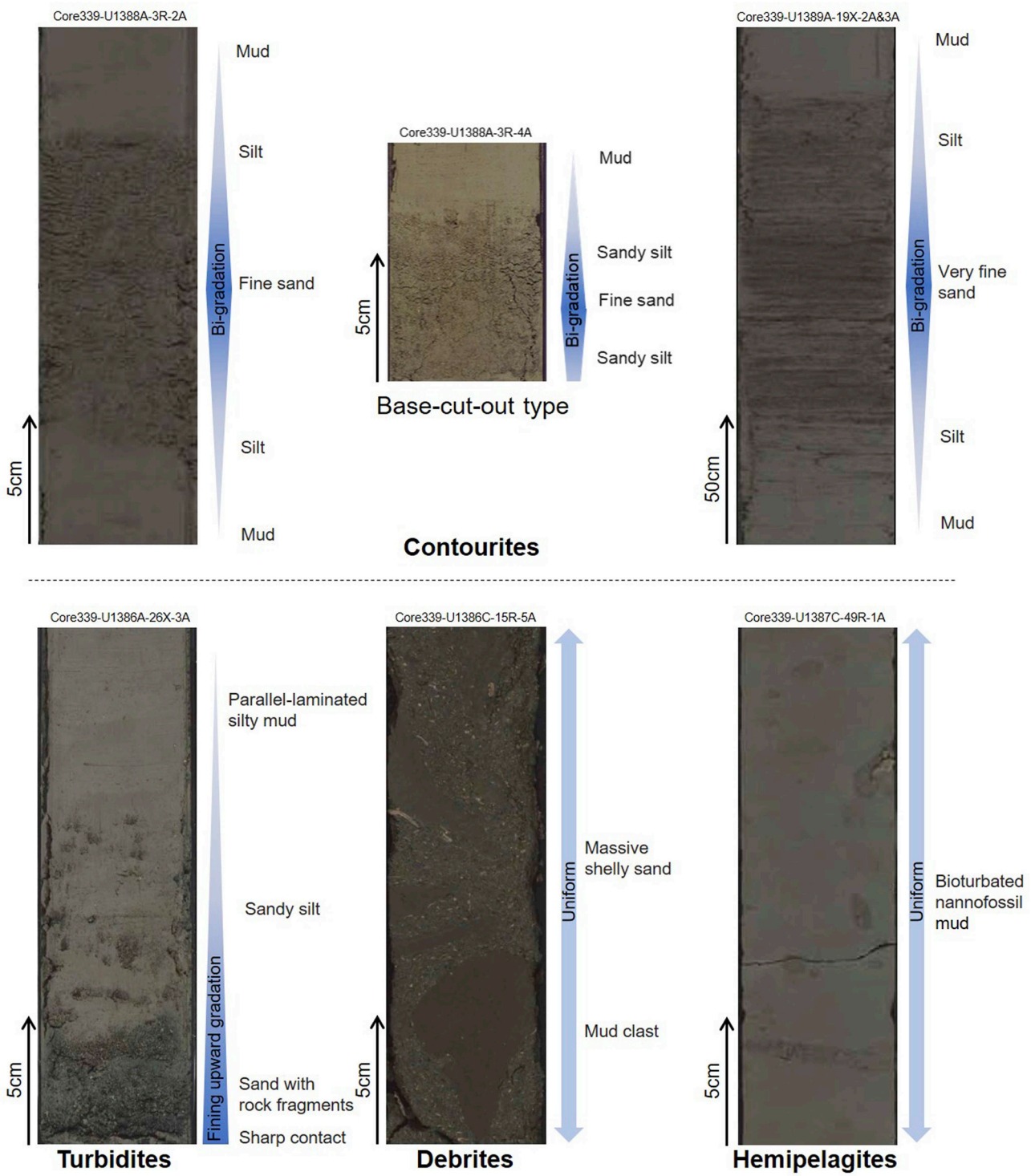

Fig. 3. Core photographs of the principal contourite, turbidite, debrite and hemipelagite facies recovered IODP 339 sites in the Gulf of Cadiz. Bi-gradational and partial contourite sequences as shown.

interpreted as bottom-current reworked turbidites.

Below a marked hiatus at three of the CDS sites (U1386, U1387 and U1391), there is clear evidence for more common downslope sedimentation within the Pliocene. This dominates the succession older than about 4 Ma to the base of the Pliocene, but also occurs interbedded with contourites younger than around 4.2 Ma. The downslope facies are characterized by a mixed and exotic composition that includes shelf-derived, fragmented macrofossils and benthic microfossils, as well as some glauconite and a higher proportion of opaque heavy minerals and lithic grains. The turbidites show clear normal grading from sand to mud above a sharp, erosive base, but mostly lack other sedimentary structures, except for some with parallel lamination. Debrites are chaotic, with contorted slump folds, isolated large clasts, and common shell debris in a sandy, muddy matrix.

The porosity and grain size data presented below are all from the contourite facies. These sediments are remarkably uniform in their mixed siliciclastic-biogenic composition and textural attributes. They have a general absence of primary sedimentary structures, except for a

somewhat discontinuous and widely-spaced silt lamination within muddy contourites that show the highest rates of sedimentation (Site U1390). There is an intense, continuous bioturbation throughout with a distinctive, small-scale, monotonous ichnofacies and local omission surfaces. Most sections are characterized by bi-gradational sequences from inverse to normal grading, but also include a range of partial sequences of which the base-cut-out sequences are most common (Fig. 3). All these features are fully consistent with the established facies model for fine and medium-grained contourites (Stow et al., 2002b; Stow and Faugères, 2008).

Spatial distribution of the contourite elements along the Cadiz continental margin are closely linked with the decrease in bottom-current speed down-flow from the exit of the Gibraltar Gateway (Stow et al., 2013b; Hernandez-Molina et al., 2014; Hernández-Molina et al., 2016b). The rocky substrate west of Gibraltar gives way to an extensive contourite sand sheet, which extends along a mid-slope terrace for approximately 100 km before diverging into several contourite channels around the prominent seafloor relief created by mud volcanoes and diapiric ridges. Seismic data and one industry borehole (Buitrago et al., 2001) indicate that this sand sheet is at least 800 m thick. Site U1388 penetrated 220 m of this proximal sand sheet, before the hole became too unstable to continue, and recovered rapidly-deposited, late Quaternary, sandy contourites. The areal extent and vertical thickness of these clean contourite sands display ideal reservoir characteristics, were they to be more deeply buried, and are therefore especially significant for the oil and gas industry.

3.2. Grain-size characteristics

The 350 new grain size analyses presented here are all from contourites recovered in four of the IODP 339 wells (U1386, U1387, U1388 and U1389). These are plotted together with the 675 analyses of box core and piston core samples (BC05, PC08, PC04, PC06) previously recorded by Brackenridge et al. (2018), thereby yielding the largest contourite grain-size set yet published (Fig. 4). The grain-size parameters measured – mean size, sorting, skewness and kurtosis – are presented as cross-plots of mean-size vs sorting (Fig. 4A), mean-size vs skewness (Fig. 4B), and mean size vs kurtosis (Fig. 4C).

The data show a wide range of values in all the measured parameters. Mean grain size ranges from clay to coarse sand (2 μm–1200 μm, or 9 phi to 0 phi), standard deviation (i.e. sorting) from very well sorted to very poorly sorted (σ 0.45 to 3.06 phi), skewness from very fine skew to very coarse skew (+0.7 to −0.6 phi), and kurtosis from very platykurtic to very leptokurtic (0.5–2.6 phi). Grain-size of the sediment cores PC04, PC08, U1386, U1387 and U1389 are mainly from clay to very coarse silt, whereas parts of cores PC06 and U1388 contain much more sand, and core BC05 is mostly dominated by fine to coarse sand. Overall, fine to coarse sands have better sorting than clay and silt grain sizes.

Each of the different cross-plots shown (Fig. 4) reveals a more or less sinusoidal variation of parameters. The best sorted sediments are fine and very fine sand in U1388 and PC06, whereas the least well sorted are very coarse silt in cores U1386, U1387, U1388 and U1389. The sinusoidal trend (Fig. 4A) shows a decrease in sorting from clay to coarse silt (9–5.5 phi), an increase from coarse silt to fine sand (5.5–2.5 phi), and a decrease from fine sand to coarse sand (2.5–0 phi). However, the trend is not everywhere so well-defined. The coarser grain sizes show more scattered sorting, as do the mean grain sizes from ~6.5 phi to ~4.5 phi and σ value from ~3.05 to ~2.3. Part of this scatter is due to slightly different trends at different sites.

The mean-size vs skewness sinusoidal curve (Fig. 4B) is offset from the mean-size vs sorting curve. Skewness defines the symmetry of the grain-size distribution curve, such that the skewness value of a normal distribution is 0. The lowest values (coarse and very coarse skew, −0.6) are at around 6.5 and 1.5 phi, with high values (very fine skew, +0.7) around 4 phi. Most of data points lie between grain sizes of ~7.5 to 6

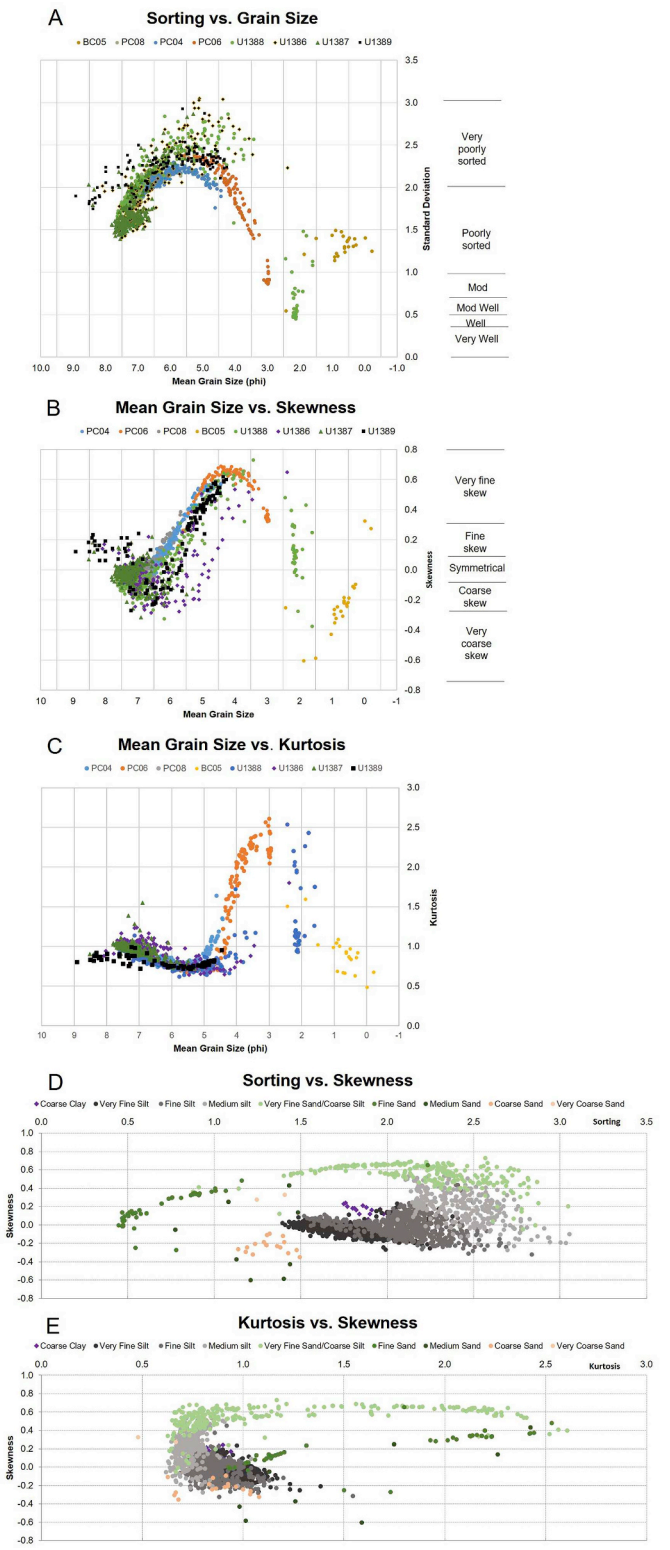

Fig. 4. Grain-size parameters cross-plots of over 1000 samples from Gulf of Cadiz contourites. Cores BC05, PC08, PC04 and PC06, after Brackenridge et al. (2018); samples from IODP 339 sites U1386, U1387, U1388 and U1389, new for this study. (A) mean grain size versus sorting, (B) mean grain size versus skewness, (C) mean grain size versus kurtosis indicate finest and coarsest sediments have similar kurtosis, (D) sorting versus skewness, (E) kurtosis versus skewness. A-C indicate sites from which samples are derived; D-E indicate grain-size classes of each sample plotted.

phi (fine to coarse silt) and skewness between ~0.1 and −0.2. Sediments with the finest skewness are very coarse silt to very fine sand, whereas medium and coarse sand has the coarsest skewness. Most of the normal distributions with very low or zero skew are observed in very fine silt to coarse silt sediments, and a very few can be found in fine sands.

The plot of mean grain size versus kurtosis (Fig. 4C) is less clearly sinusoidal. Kurtosis defines the degree of peakedness of the distribution curve, more concentrated if they have leptokurtic distribution, and more dispersed if they have platykurtic distribution. The finer grained sediment, clay to coarse silt (9–4.5 phi), are mainly mesokurtic and platykurtic, with the lowest values at around 5.5 to 4.5 phi. From coarse silt to fine sand (4.5–3 phi), sediments show a rapid change from platykurtic to very leptokurtic, and then a marked decline from fine to coarse sand (3–0 phi) to very platykurtic distributions.

Plots of sorting versus skewness and kurtosis versus skewness are also shown in Fig. 4D and E, with the data points arranged in grain size classes rather than by site. These relationships are quite complex, but do serve to illustrate at least three distinct grin-size clusters with an elongate trend: (a) clay to fine silt (purple, black and dark grey points) with poor to very poor sorting (1.5–2.5 phi), zero to low skewness (+0.2 to −0.2 phi), and platykurtic distribution; (b) medium silt to fine sand (light grey and green points) with very poor to good sorting (2.75–0.5 phi), zero to coarse-tail skew (0 to −0.6 phi), and very platykurtic to leptokurtic distribution (0.6–2.5 phi); and (c) medium to coarse sand (dark green and pink points) with poor to good sorting (1.5–0.5 phi), zero to very coarse-tail skew (0 to −0.7 phi), and platykurtic to leptokurtic distribution (0.6–2.5 phi).

3.3. Porosity profiles

We first present porosity-depth curves for the four Gulf of Cadiz wells (Fig. 5), and then selected data from other contourite drift systems for comparison (Fig. 6).

3.3.1. Gulf of Cadiz contourites

The porosity-depth profile at site U1386 is shown in Fig. 5. The sediments above 420 m depth are exclusively contourites, whereas below this they become interbedded with turbidites. According to this profile, the overall porosity range is between 34 and 58% (with three outlier data points), and slowly decreases from ~50 to 60% at the top to ~40–45% at the base of the well. The data points appear more scattered below 300 m, which corresponds to the beginning of slight and dispersed cementation. Although there are relatively few sandy contourites present, we can discern different sub-trends for muddy and sandy contourites as indicated by the yellow and green trend lines, respectively. The porosity of muddy contourites gradually decreases in the first ~170 m, and then increases slightly before decreasing again with a faster rate up to a depth of ~270 m. There is little further change below ~270 m so that the average porosity of mud remains at ~40–45%.

The trend line of porosity with depth for silty sands (based on five data points) shows a decrease from 45% at 20 m depth to around 35% at over 400 m depth. The sands and sandy silts below 400 m are somewhat anomalous, with porosity values of 40–50%.

The porosity profile of site U1387 is shown in Fig. 5. Contourites are the principal facies above ~460 m, after which they are interbedded with turbidites and related facies. The porosity-depth trend for contourites shows an overall porosity between 37 and 58%, with three outlier points in sandy sediments, which are most likely due to cementation (Stow et al., 2013a). The average porosity is ~50–60% at the top and decreases to 40–45% at the bottom, with three sub-trends. Porosity data for sandy contourites is insufficient to present any distinct trend. The porosity of mud contourites reduces to ~44% at a depth of ~340 m, increases by approximately 4% over the next ~110 m interval, and then decreases again at a similar rate as the topmost section. There are possible breaks in these trends at around 400 m and at 700 m.

The amount of porosity data gathered from site U1388 is much less than from the other sites, due to the difficulty of core recovery within these coarser-grained sediments (Stow et al., 2013a). However, there are some interesting trends apparent in the 250 m of section recovered (Fig. 5). The porosity lies between 38 and 52% for muddy contourites and relatively lower, 42–48%, for sandy contourites. Both show an initial decrease with depth ~150 m interval, and then a marked break in trend and slight increase to 47%.

Overall range of porosity at site U1389 is mainly between 35 and 58%, as shown in the porosity-depth profile, with 5 outlier points (Fig. 5). The porosity in three samples near the top is 60–70%, but rapidly decreases to 45–55% at the depth of tens of meters, and then gradually decreases to 35–45% at a depth of ~300 m. There is a distinct break in trend associated with a minor hiatus at this depth, after which the values jump higher by 4–5%, and then proceed to decrease from ~49% to ~43% at a similar rate as the topmost interval. The very low value at around 500 m is due to cementation, whereas the anomalously high value at 600 m has no clear explanation. The trend in sandy contourite porosity values is from 55 to 38%, at a similar rate of decrease to the muddy contourites.

3.3.2. Other contourite porosity profiles

To compare the porosity characteristics of contourites from the Gulf of Cadiz with those of different settings, we selected four sites from other IODP expeditions – site U1305 (IODP 303) on the Eirik drift, site U1304 (IODP 303) on the Gardar drift, site U1410 (IODP 342) on the Newfoundland drift, and site U1352 (IODP 317) on the Canterbury slope. Sites U1410 and U1305 from the Newfoundland and Eirik drifts are at significantly greater water depths, in excess of 3000 m, than those sites from the Gulf of Cadiz, whereas water depth of site U1352 on the Canterbury slope is a little shallower, but the depth of penetration below the seafloor is much greater – close to 2000 m burial depth (Table 1). Sediments of all these sites are less sandy than those of IODP 339 and also generally more carbonate-rich (Channell et al., 2006; Fulthorpe et al., 2011; Norris et al., 2014).

Eirik Drift: Site U1305 is located south of Greenland and drilled on the south-western border of Eirik drift, which was generated by Norwegian Sea Overflow Water during Pliocene and Quaternary (Channell et al., 2006). The sediments consist of mixed terrigenous, biogenic and detrital carbonate material, deposited during Pliocene to Pleistocene. At this site, the lithology is very uniform, predominantly silty clay with a relatively small amount of nannofossil ooze and sandy clay, and no sandy contourites. The majority of samples show porosities between 50% and 77% (Fig. 6), with two notable outliers. The original porosity is relatively high (~74–77%), and decreases with depth to around 50–53% at the bottom (~230 m depth). There is some irregular oscillation apparent in this overall trend.

Gardar Drift: Site U1304 is located on the eastern flank of the Mid-Atlantic Ridge, south of Iceland in the North Atlantic. Sediment recovery is from Late Pliocene to Holocene, and consists of interbedded nannofossil ooze and diatom ooze with silty clay (Channell et al., 2006). The porosity data points are relatively scattered (Fig. 6). The range of overall data points is from 68% to 87% with one obvious outlier. The original porosity is very high, around nearly 80%, and there is almost no marked decrease to the bottom of the hole (~240 m depth).

Newfoundland Drift: Site U1410 is located on the Newfoundland ridge, North Atlantic, and recovered sediments from the Paleogene-Recent Newfoundland drift (Norris et al., 2014). It is divided into four different lithological units: Unit I (0–34 m) is mixed clay sediments and foraminiferal ooze, Unit II (34–64 m) mainly has clay sediments with some nannofossil ooze, Unit III (64–211 m) is dominated by clay and nannofossil ooze, and Unit IV (211–258 m) predominantly chalk and claystone. Overall, the porosity decreases from an average of 70–75% at the top to around 40–45% at the bottom (Fig. 6). There is a marked porosity decrease by 10–15% in the first 50 m interval, and then there

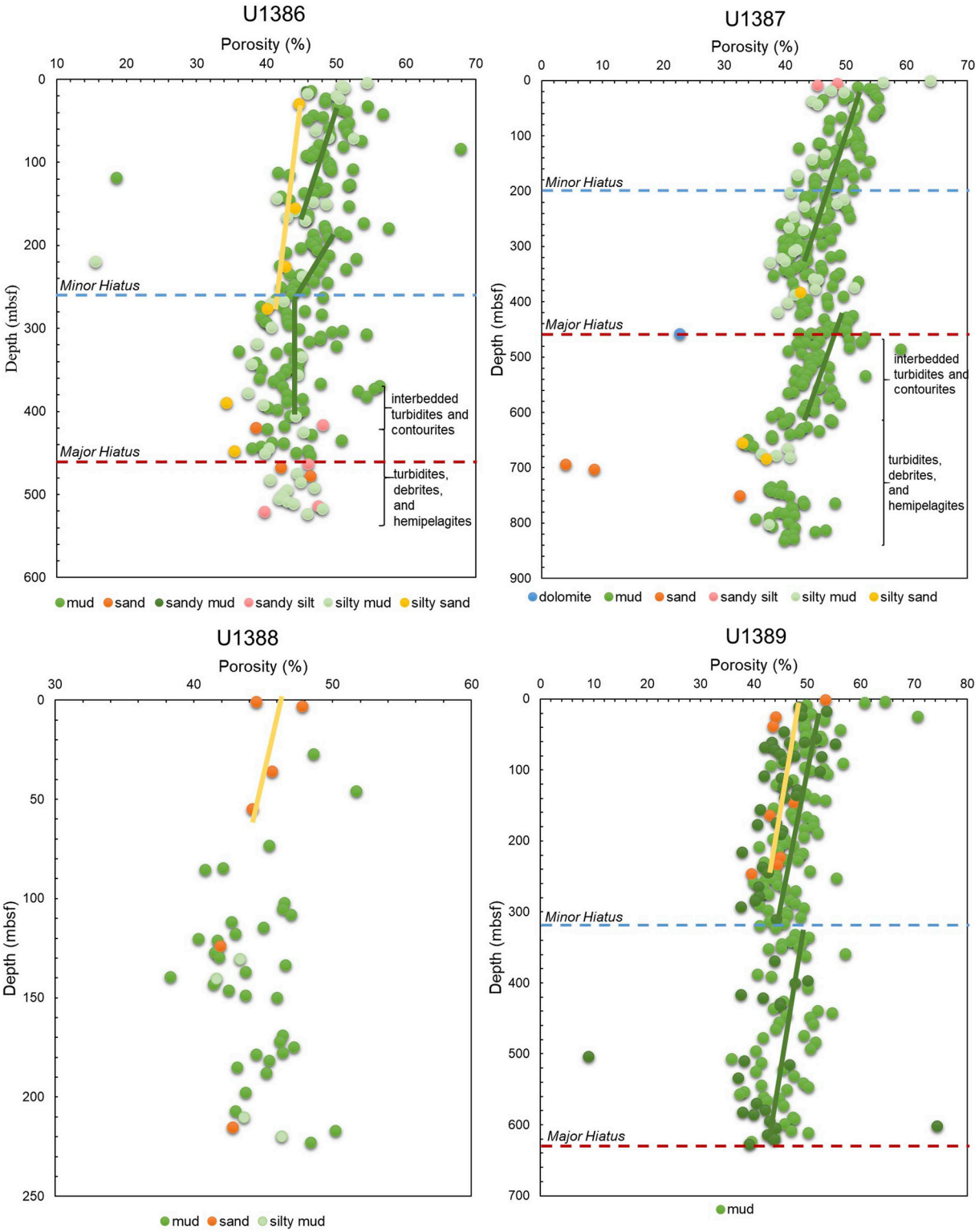

Fig. 5. Porosity-depth profiles for sites U1386, U1387, U1388 and U1389. Because of problems with core recovery of sandy sediments, U1388 has much less data points than the others. Different sites are shown in different colours. The green and yellow lines are estimated trends for mud and sand respectively. These are mostly contourite facies. Below about 400 m at sites U1386 and U1387 (see Fig. 2) the succession comprises interbedded contourites, turbidites, debrites and hemipelagites. Blue and red dashed lines show the minor hiatus and major hiatus in U1386, U1387 and U1389 respectively. (For interpretation of the references to colour in this figure legend, the reader is referred to the Web version of this article.)

only a very slight decrease down to 170 m. The rapid decrease from 170 m appears to be linked to compaction and early cementation of clay and ooze resulting in the formation of claystone and chalk.

Canterbury Slope: Site U1352 is located on the upper slope of Canterbury Bight, New Zealand, and recorded sediments deposited during late Eocene to early Oligocene (Fulthorpe et al., 2011). It is divided into three main lithological units, which mainly consist of interbedded clay and mud, sandy mud, and muddy sand. There is more

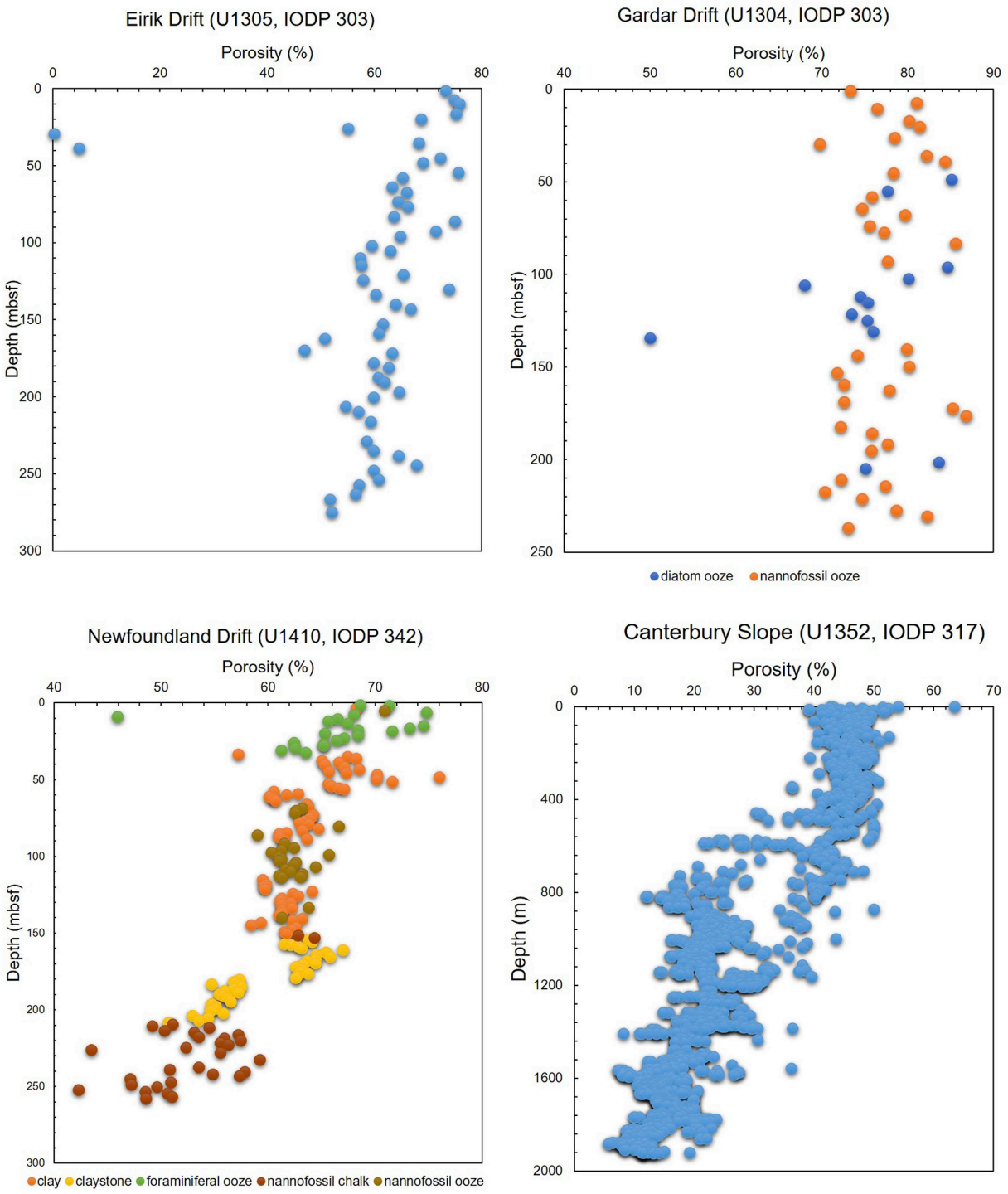

Fig. 6. Porosity-depth profiles of Eirik drift (U1305, IODP 303), Gardar drift (U1304, IODP 303), Newfoundland drift (U1410, IODP 342) and Canterbury slope (U1352, IODP 317). Sediments types of Newfoundland drift are showing in different colours. (For interpretation of the references to colour in this figure legend, the reader is referred to the Web version of this article.)

siliciclastic content in the upper part and more carbonate in the lower part. The three lithological units are: Unit I (0–711 m) is dominated by mud-rich sediments and interbedded sand; Unit II (711–1853 m) mainly consists of uncemented sandy mud and cemented sandy marlstone; and Unit III (1853–1924 m) consists of cemented sandy and silty limestone. The porosity-depth profile is relatively more marked at this site because of the relatively deeper burial depth compared with contourites of the other sites considered. The porosity range at the surface is ~40–56%, with one value of 65%, whereas the average porosity at the base is 4–14% (Fig. 6). There is a modest decrease in porosity in the upper 500 m interval, but with the beginning of cementation from 500 m, the porosity points are more scattered, and the porosity decreases more rapidly from 40% to 25% in the next 400 m interval. Below that, the porosity gradually decreases with depth from 900 to 1850 m to around 4–14%.

Table 2
Parameters for the normal exponential porosity-depth equation (Rubey and Hubbert, 1959; Sclater and Christie, 1980).

Lithology	Original porosity (f_0)	Compaction coefficient (c)
Sandstone	0.49	0.27 × 10-3 m^{-1}
Mudstone	0.63	0.51 × 10^{-3} m^{-1}

3.4. Exponential models of the porosity-depth relationship

The porosity-depth relationship is the principal factor to be considered for evaluating the reservoir potential of any particular sedimentary succession or facies. Rubey and Hubbert (1959) established a general exponential equation for the porosity-depth relationship under normal pressures, which they formulated as:

$$f = f_0 e^{-cz}$$

(where f = porosity at normal pressure, f_0 = original porosity, e = natural logarithm, c = compaction coefficient, z = depth).

Using this equation, Rubey and Hubbert (1959) analysed the porosity-depth exponential relationship of shale and mudstone, whereas Sclater and Christie (1980) found the exponential relationship for sandstone by studying North Sea reservoirs. The parameters from these previous studies can be used as the normal values for sand and mud (Table 2).

According to these previous studies, therefore, the exponential porosity-depth models can also be derived from porosity data of the study area as presented above. The parameters used in the exponential equations are presented in Table 3, showing values for mud and sand facies separately. Insufficient sandy contourite values from Site U1387 precludes developing the exponential equation in this case.

Using these models, the exponential curves have been drawn and shown in comparison with the curves for mud and sand under normal compaction pressure. These show predicted trends of porosity change with depth for each of the Gulf of Cadiz sites (Fig. 7). It should be noted that these curves simply provide an approximation of likely trends in porosity-depth curves, with predicted values extended to a depth of 2500 m. Note that the porosity predictions are based solely on the exponential equations derived from IODP 339 data. The actual values will be subject to a range of more complicating variables, such as differential cementation, long-duration hiatuses in the sediment record, and so on.

Contourite muds: The exponential curves of porosity for sites U1386 and U1389 each show trends comparable with that for normal mud. Due to the locally increasing porosity intervals of U1387 and U1388, these curves indicate an increasing trend, so that the exponential curves of these two sites are invalid. The original porosity (f_0) of U1386 of around 50% is ~13% less than that of normal mud, but by reason of its lower compaction coefficient, the rate of porosity decrease for U1386 is relatively slower, so that by 2500 m depth, the predicted porosity of U1386 is very close to that of normal mud - at about 18%. A similar result is apparent for site U1389, for which the exponential model predicts a decrease from 50% at the surface to ~24% at 2500 m depth, or about 6% higher than that for normal mud.

Contourite sands: With relatively less data points available (and none for U1389), the exponential curves for contourite sand porosity are less robust. From a surface porosity of between 45 and 55%, each of the three sites is predicted to decrease to between 10 and 17% at 2500 m depth. These exponential porosity curves compare with that for normal sand, which decreases from 49% to 25% at 2500 m.

Table 3
Parameters and exponential equations derived from IODP339 data.

Site	Original porosity(f_0)	Compaction coefficient (c)	Equation
Mud:			
U1386	0.4937	0.4 × 10^{-3} m^{-1}	$f = 0.4937e^{-0.4\times10^{-3}(-3)z}$
U1387	0.4457	0.2 × 10^{-3} m^{-1}	$f = 0.4457e^{-0.2\times10^{-3}(-3)z}$
U1388	0.4406	0.6 × 10^{-3} m^{-1}	$f = 0.4406e^{-0.6\times10^{-3}(-3)z}$
U1389	0.4958	0.3 × 10^{-3} m^{-1}	$f = 0.4958e^{-0.3\times10^{-3}(-3)z}$
Sand:			
U1386	0.4716	0.6 × 10^{-3} m^{-1}	$f = 0.4716e^{-0.6\times10^{-3}(-3)z}$
U1387	–	–	–
U1388	0.4578	0.4 × 10^{-3} m^{-1}	$f = 0.4578e^{-0.4\times10^{-3}(-3)z}$
U1389	0.4797	0.5 × 10^{-3} m^{-1}	$f = 0.4797e^{-0.5\times10^{-3}(-3)z}$

4. Discussion

4.1. Grain size of contourites

Grain size parameters are one of the fundamental characteristics of sediments, strongly linked with sedimentary environment, sediment supply, current energy and depositional process. Sediment texture is also a key attribute for assessing the nature of reservoirs and seals in the subsurface. There have been many hundreds of publications on sediment textures over the past six decades, since some of the early work that focussed largely on continental sedimentary environments (Folk and Ward, 1957; Mason and Folk, 1958; Martins, 1965; Pollack, 1961; Friedman et al., 1992). Important syntheses of this work, including marine and deep marine environments, are published in a number of key sedimentology texts (Blatt, 1992; Friedman et al., 1992; Leeder, 1999; Stow, 2005; Bridge and Demicco, 2008; Boggs, 2009). The strong link between grain size and porosity-permeability characteristics is highlighted by Selley (2000), and Gluyas and Swarbrick (2004), amongst others. However, there are still relatively few papers documenting the grain-size characteristics of contourites and almost none that are directly linked with reservoir potential (Stow and Holbrook, 1984; Stow and Faugères, 2008; Mulder et al., 2013; Brackenridge et al., 2018).

This last paper (Brackenridge et al., 2018) is a particularly important synthesis of grain-size data from the Gulf of Cadiz contourites, based mainly on gravity and box core samples from near-surface sediments. We have incorporated these data with our new grain-size analyses from the IODP wells, and the expanded cross-plots of grain-size parameters clearly re-inforce the validity of relationships and sinusoidal trends established previously. The new data points greatly extend information on clay to coarse silt, and some very fine sand contourites. We further develop the interpretation and discussion below, with reference to a simplified overlay of the three cross plots – mean size vs sorting, mean size vs skewness, and mean size vs kurtosis (Fig. 8A). Using the mean size vs sorting as a base, we define three main contourite types as follows (Fig. 8B).

Clay to fine silt contourites: These very fine-grained contourites (mean 9 to 5.5 phi, 2–20 μm) show a general poor to very poor sorting trend, low to zero skewness, and a platykurtic distribution. These characteristics are compatible with deposition in the absence of current control (i.e. hemipelagic deposition) to that beneath very weak bottom currents (< 10 cm/s). Much of the material will have been transported as larger flocs, so that the disaggregated grain-size character illustrated here is difficult to fully interpret. The broad scatter of points as well as the clustered trends from individual sites are most likely due to intensive bioturbational mixing, as well as to different proportions of principal components, as suggested by the platykurtosis.

Medium silt to fine sand contourites: This range of contourite grain sizes (mean 5.5 to 2.25 phi, 20–200 μm) are strongly influenced by bottom-current deposition and winnowing. We refer to the distinctive trends of grain-size parameters (Fig. 8) as the standard *contourite depositional trend.* These are from very poor to well-sorted, zero to fine-tail to coarse-tail skewness, and from very platykurtic to leptokurtic. Overall, sorting of coarser sediments is better than finer sediments. We concur with Brackenridge et al. (2018) that the finer sediments within

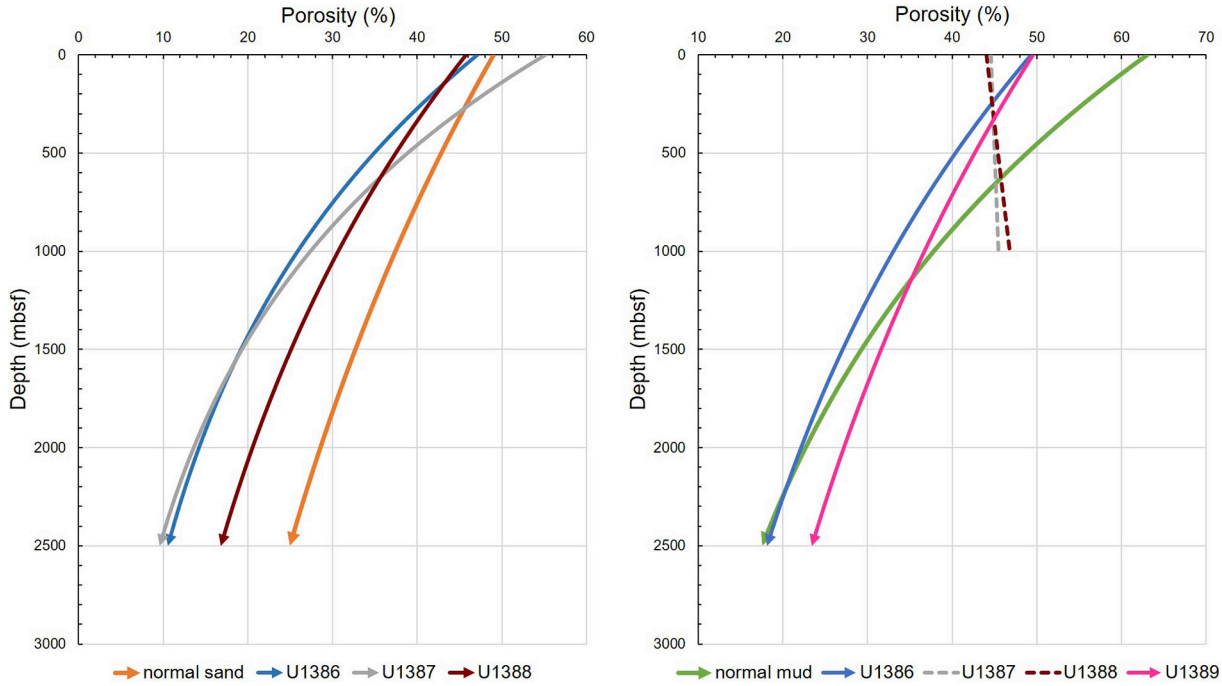

Fig. 7. Exponential models for porosity-depth profiles of sand (A) and mud (B) contourites, derived from porosity data of U1386, U1387, U1388 and U1389. Predictions are made to likely reservoir depths of 2500 m, although the actual porosity data for these sites is between 250 and 850 m depth. The parameters of normal sand and mud are provided after Rubey and Hubbert (1959) and Sclater and Christie (1980). Because of the lack of sand porosity data for U1389, only sand porosity models of U1386, U1387 and U1388 are derived. Due to some anomalous porosity values (i.e. increasing trends) in U1388 and U1389, the exponential curves cannot be derived for these sites.

this range are mainly deposited from suspended load, whereas the saltation load becomes progressively more prevalent as the grain size increases from coarse silt to fine sand. The change from fine-tail to coarse-tail skewness follows this trend, and indicates transition from a deposit controlled principally by the maximum carrying capacity of the current (10–20 cm/s), to one affected by progressive winnowing at higher current speeds (15–25 cm/s).

Medium and coarse sand contourites: These purely sandy contourites (mean 2.25 to −0.5 phi, 200–1250 μm) are strongly influenced by bottom current action. They show a general trend in grain-size parameters, with some degree of scatter, from well to poorly sorted, coarse and very coarse-tail skew to zero skew, and from mesokurtic to platykurtic. Strong current winnowing, and grain saltation is augmented by widespread bedload traction, which increases in importance with increase in grain-size. The suspended load is swept downstream from the depositional site. The greater scatter of data points in this sector is due to innate variability in current speed, and a distinctly mixed supply of different source material, both siliciclastic and bioclastic.

These interpretations of the different contourite grain-size classes are compatible with work by previous authors (Allison and Ledbetter, 1982; Brunner, 1984; McCave, 1984; Viana et al., 1998; Faugères and Mulder, 2011; Alonso et al., 2016; Brackenridge et al., 2018). Our three classes can be related to the contourite end-member models proposed by Brackenridge et al. (2018) as follows: clay to fine silts (model B), medium silt to fine sand (models C and D), and medium to coarse sands (model A). The principal controls on these textural properties are: current speed, sediment supply, flocculation, and bioturbation. We make a few further observations on the first two of these controls.

Current speed: The link between contourite grain size and bottom-current speed has long been recognised (Ledbetter and Ellwood, 1980; McCave, 1984, 2008), and is proposed as the principal control to explain the standard bi-gradational sequence model for contourites (Gonthier et al., 1984; Stow et al., 2002b; Stow and Faugères, 2008). The (de-carbonated) grain-size fraction between 10 and 63 μm, known as *sortable silt (SS)*, is commonly used as a proxy for current speed (McCave et al., 1995; McCave, 2008). However, the sortable silt size range currently used matches only one trend on the mean size vs skewness (Fig. 8), whereas the distinctive contourite depositional trend, which we identify in this paper from the grain-size vs sorting cross-plot, is from 20 to 200 μm. We therefore propose that a new sortable silt and sand proxy (SSS) should be developed to better reflect the full grain-size range that is strongly controlled by current speed. Work is currently in progress on this topic.

Sediment supply: The sediment source and supply route also have a significant influence on grain-size properties. For contourite systems, there can be supply from vertical settling of pelagic material, slow hemipelagic advection, lateral input from turbidity currents, and directly from the bottom currents via local or more distant seafloor erosion. Stow et al. (2008) attempt to constrain an overall sediment budget from these different sources for a 'typical' contourite drift, but readily acknowledge that different drifts and different parts of the same drift will receive material from these sources in varying proportions.

For the Gulf of Cadiz contourites documented in this paper, we interpret the broad scatter of data points as in part due to different sedimentary material from a range of sources. This is especially true for the finest (clay-silt) and coarsest (medium-coarse sand) contourites for which current speed is not the sole or principal control on grain size. The locations of sites U1388, BC05, PC04, PC06 and PC08 are much closer to Gibraltar gateway than U1386, U1387 and U1389 (Fig. 1), and are therefore affected by both different current speeds and different sediment supply. Brackenridge et al. (2018) pointed out samples from PC04 and PC06 have parallel but separated trends, which they interpret as sediment supplied to PC04 from the Southern Channel, which transports sediments from the Gibraltar gateway and its adjacent margins, and sediment supplied to PC06 mainly from downslope processes. We note similar partial separation of trends for sites U1386, U1387 and U1389.

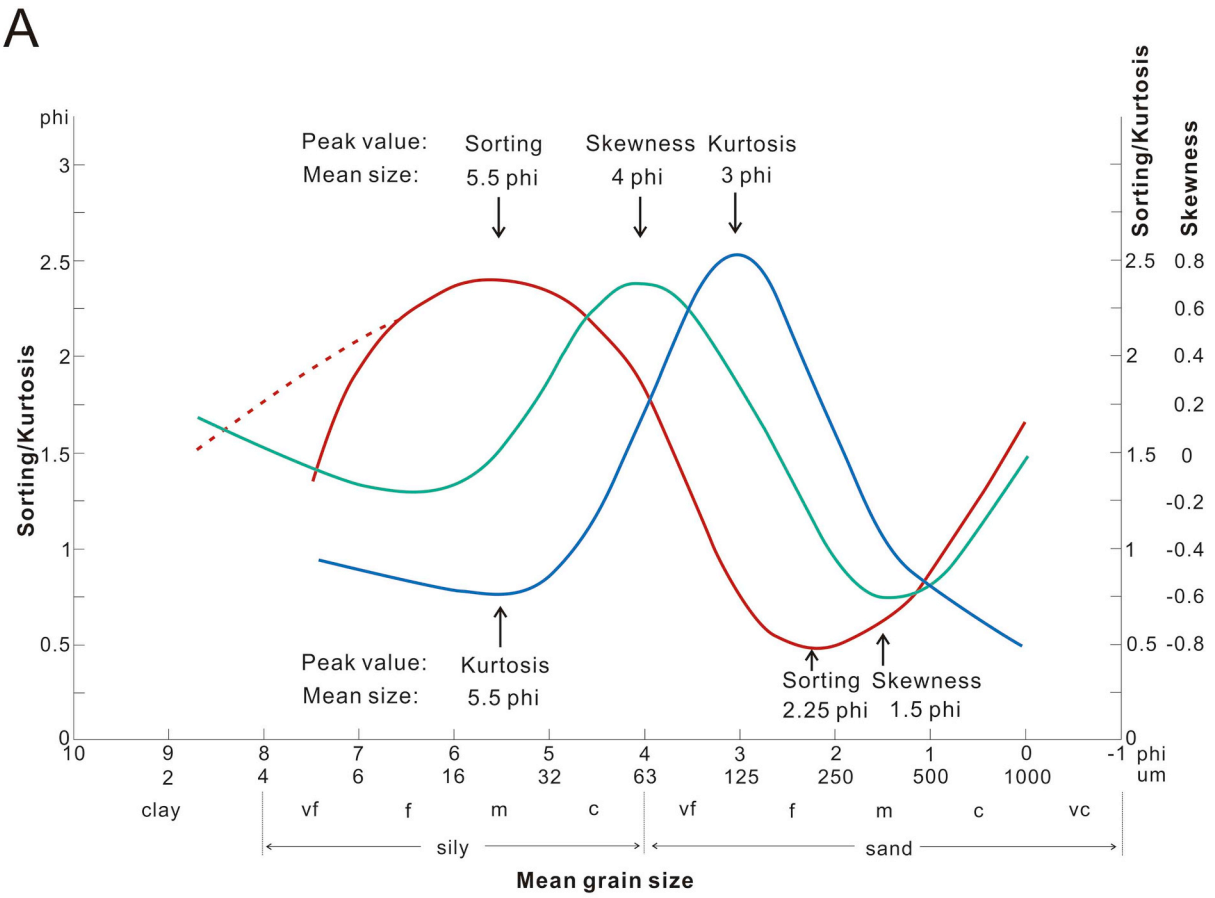

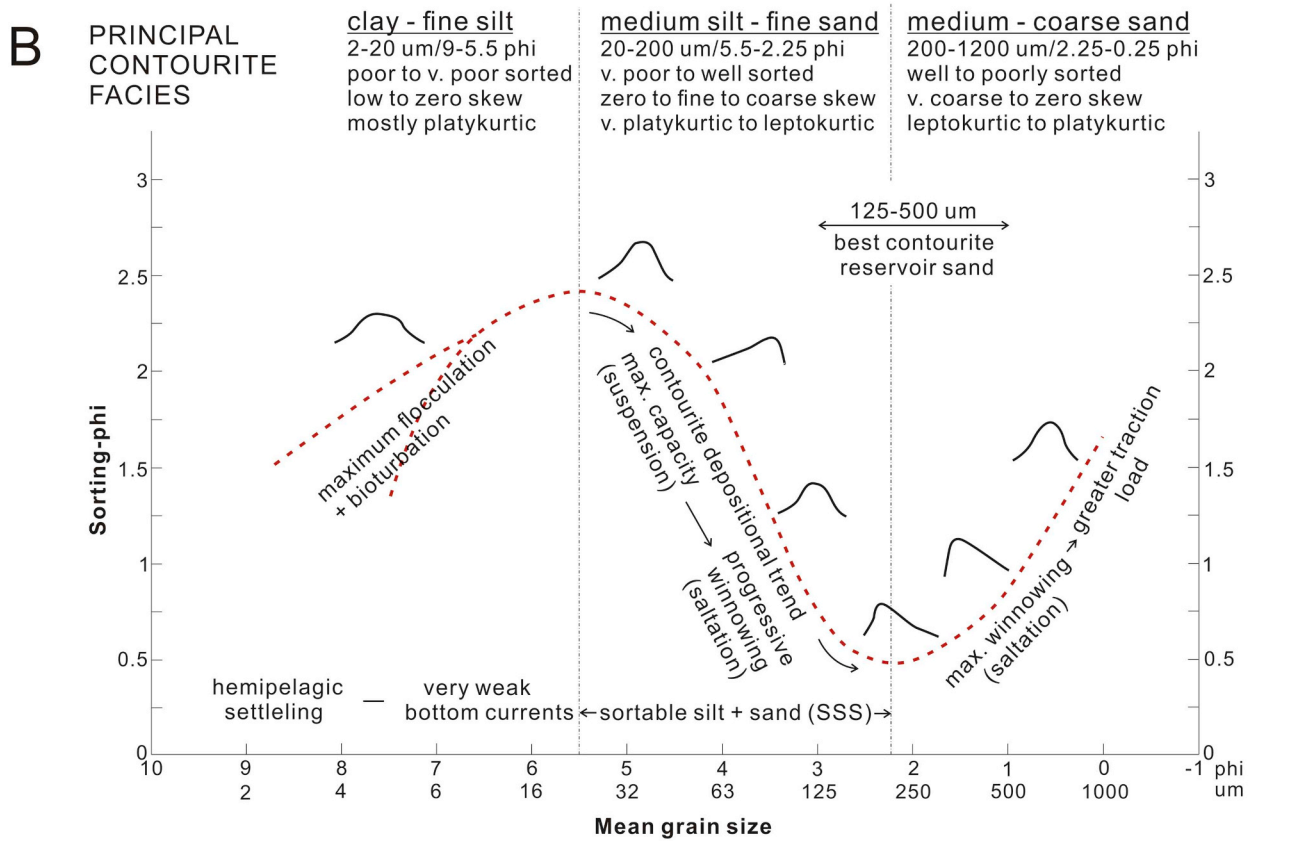

(caption on next page)

Fig. 8. Summary grain-size cross plots and their interpretation. (A) Schematic representation of best-fit trend lines for mean size vs sorting (red), mean size vs skewness (green), and mean size vs skewness (blue). Upper peak values show mean grain size for poorest sorting, most fine-tail skew, and most leptokurtic distribution. Lower peak values show mean grain size for best sorting, most coarse-tail skew, and most platykurtic distribution. (B) Schematic representation of best-fit trend line for mean grain size vs sorting (as above), noting grain-size attributes of the three principal facies classes of contourites, and the inferred depositional processes for each. The small curves adjacent to the trend line illustrate the general shape of grain-size distribution curves at different points along the line. . (For interpretation of the references to colour in this figure legend, the reader is referred to the Web version of this article.)

4.2. Porosity-depth relationships

For the Gulf of Cadiz contourites, both the actual data plots and the exponential porosity-depth curves show some significant departures from the normal trends for sand and mud, as proposed by Rubey and Hubbert (1959) and Sclater and Christie (1980) under normal conditions of pressure. In particular, the Cadiz sites, (a) have lower porosity values at the surface, and (b) show irregularities and breaks in the porosity depth profiles. In general, porosity decrease is mainly dominated by the mechanism of physical compaction above ~500 m burial depth, through which grain rearrangement accommodates to the overlying pressure (Athy, 1930; Busch, 1989). Below 500 m, porosity reduction takes place as a response to a combination of compaction, cementation and dissolution.

There are several possible factors that may have led to the abnormal porosity profiles for the Cadiz contourites. Firstly, the primary porosity of surface sediments may be different where deposited under the persistent influence of bottom currents, perhaps as a result of different sediment fabric. This might explain the lower than normal surface porosity observed. Secondly, the parts of the depth profiles with higher than expected porosity values suggest abnormal pressure or overpressure conditions and hence the relative under-compaction of the sediments (Fig. 9).

This condition can arise during sediment compaction where pore fluids cannot readily escape or the fluid expulsion rate is very low (Osborne and Swarbrick, 1997; Waples and Couples, 1998). High sedimentation rates (> 10cm/ka) of fine-grained sediment is known to lead to overpressure in many sedimentary basins in the world. Sedimentation rates for the Cadiz sites certainly meet this criterion (Stow et al., 2013a) – 15–35 cm/ka at U1386, 15–25 cm/ka at U1387, up to 60 cm/ka at U1388, and 30–40 cm/ka at site U1389.

Furthermore, dolomite cementation occurred just below the major hiatus at site U1387, and is believed to be widespread across the drift system. If this is the case, then it may act as a local seal and hence barrier to fluid expulsion and so generate overpressure and decrease the porosity reduction (Wangen, 2010). Other locally cemented or partially cemented zones may account for other areas of overpressure and porosity anomaly. Certainly, overpressure is an efficient way to preserve porosity in the subsurface (Jansa and Urrea, 1990; Stricker and Jones, 2018). Scherer (1987) estimated porosity retention of nearly 2% for every 1000 psi overpressure in sandstone reservoirs.

4.3. Comparison of porosity profiles

The porosity profiles of the Cadiz contourite sites are all quite similar, although they each show some anomalous variation and distinct profile breaks (Fig. 10). The sandy contourite site (U1388) has slightly lower porosity values on average. Comparing these with the other contourite systems documented herein reveals further interesting information. The two drift sites that are distinctly more biogenic in composition (Newfoundland drift is carbonate-rich, Gardar drift is mixed carbonate-siliceous biogenics) have significantly higher surface porosities than in Cadiz (Fig. 10B and C). The Newfoundland site also undergoes relatively early cementation, so that porosities decrease rapidly below about 170 m depth. The Eirik drift site also has higher surface porosities, which then decrease quite rapidly (Fig. 10A). This site is located on a distal part of the drift and is also relatively biogenic-rich in the upper 100 m. It seems evident that biogenic contourite systems have higher primary depositional porosity than siliciclastic and mixed drifts, and are then more prone to early and differential cementation.

By contrast, the Canterbury slope contourites have a similar siliciclastic composition and show very similar surface porosities to those of Cadiz, as well as a closely parallel trend of decrease, at least down to 860 m depth (Fig. 10D). Below that depth, the Canterbury contourites are more carbonate-rich and become more subject to variable cementation. All sites are characterised by some anomalous trends and breaks in profile, which we suggest are typical of contourite systems, especially those with widespread hiatuses and mud-rich or biogenic-rich composition.

4.4. Reservoir potential

4.4.1. Modern analogues

There is considerable interest at present in contourites as potential reservoirs, both conventional and unconventional, with some authors suggesting that they will be at the forefront of deep-water exploration in the coming decades (Shanmugam, 2006, 2012; Viana, 2008; Stow et al., 2011, 2013b; Hernández-Molina et al., 2016b). Recent studies have documented the presence and widespread extent of contourite sand sheets in slope settings. These include siliciclastic examples in the Gulf of Cadiz (Buitrago et al., 2001; Stow et al., 2013b; Brackenridge et al., 2018), Hebridean margin (Stow et al., 2002a), and on the Falkland slope (Nicholson and Stow, 2019), as well as biogenic carbonate examples on the Bahama Banks (Shanmugam, 2017) and offshore the Maldives (Lüdmann et al., 2013, 2018). These modern analogues provide good information on contourite architecture, showing extensive sand sheets covering 4000–25,000 km^2 and with thicknesses from a few tens of metres to several hundreds of metres. The sediment properties reveal both clean sands and muddy bioturbated sands, interbedded with muddy contourite intervals.

Most of the contourites documented in this study from the Gulf of Cadiz are fine grained (muds and silts), although these are interbedded in parts, especially proximal to the Gibraltar gateway, with sandy contourites. The very fine and medium sands show the best sorting characteristics, with little clay matrix, and would offer the best reservoir properties in terms of porosity and permeability when buried. These well-sorted contourite sands have been subjected to active winnowing away of fine silts and clays by moderately strong bottom currents. Coarse-grained sandy contourites are slightly less well sorted, partly as a result of intermittent bedload traction and partly due to a more mixed sediment supply. In some areas, this supply was most likely from downslope turbidity currents.

The porosity measurements reported here from the Cadiz system record the dominance of extensive muddy contourites, and rather less sandy contourites. Both show slightly lower than normal porosities (typically 50–60%) in near-surface sediments, which is around 10–15% lower than for 'normal' muds and sands. The observed decrease in the first few hundreds of metres and the predicted values from exponential porosity-depth curves for both muddy and sandy contourites indicate that they are likely to preserve good porosity values at reservoir depths – 16% for sands and 18–24% for muds at 2500 m burial depth. However, because of the commonly interbedded nature of these facies, as well as the occurrence of widespread hiatuses in contourite systems, the porosity-depth profiles are likely to show anomalies. Over-pressured zones with higher than normal porosities were observed in the

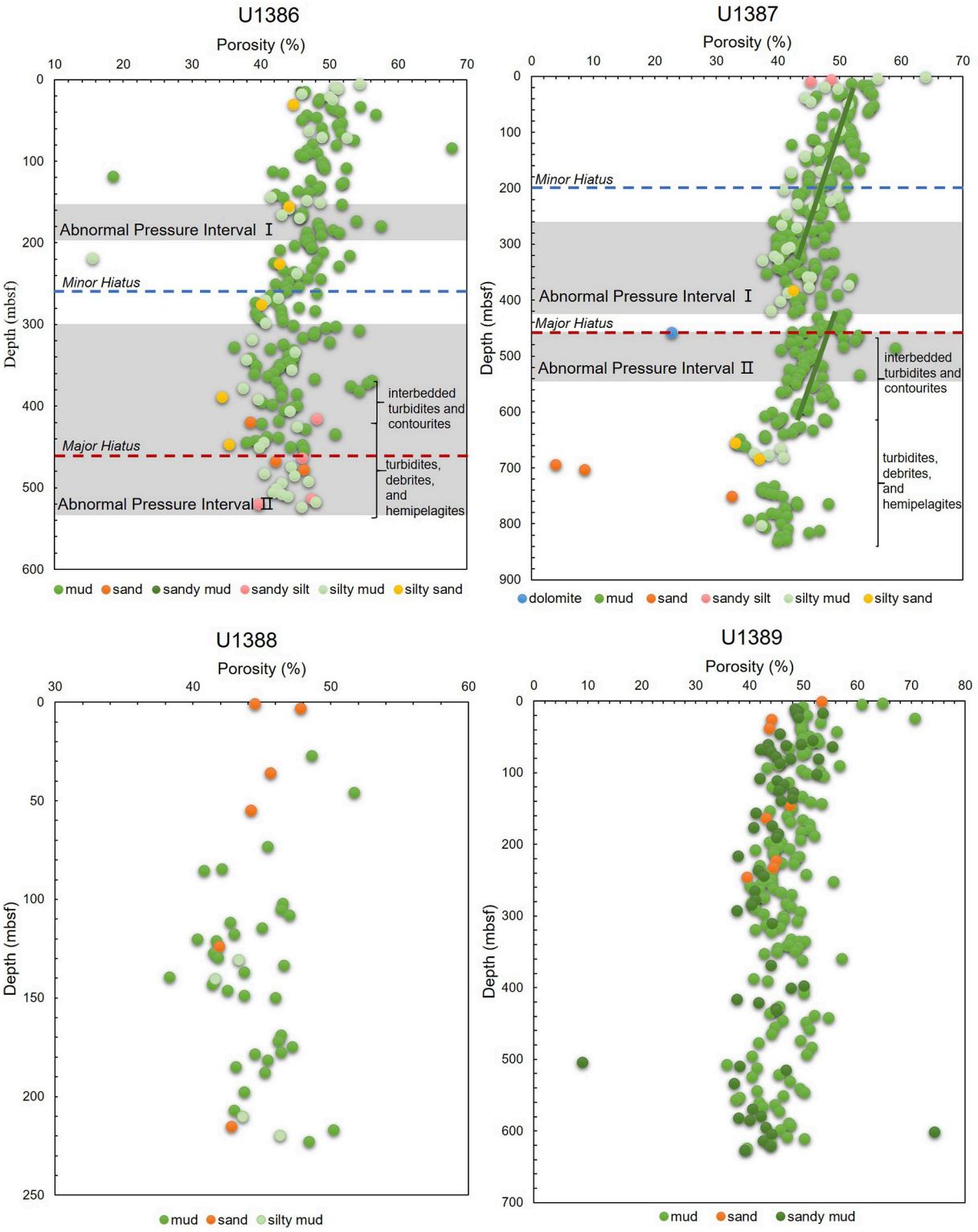

Fig. 9. Abnormal pressure intervals defined by abnormal porosity change trends are shown in the porosity-depth profiles of U1386, U1387, U1388 and U1389, indicating the occurrence of overpressure zones. This is an effective way to prevent porosity decrease during burial and retain high porosity values, at least locally.

Cadiz wells.

Comparison with porosity-depth profiles compiled from four other contourite systems confirms the patterns observed in Cadiz in the case of the Canterbury slope system, but also reveal some differences for bioclastic (carbonate and siliceous) contourites. These have higher primary porosities at the surface, but then are more subject to cementation and dissolution with depth of burial. All the contourite systems examined here show that anomalous porosity-depth profiles are most likely the norm.

Whereas we do not have permeability measurements for the mainly unconsolidated sediments presented in this study, we can use a standard porosity-permeability cross plot for different grain sizes (Chilingar, 1964) in order to infer likely permeabilities of our contourite sediments in the subsurface (Fig. 11). Taking an average

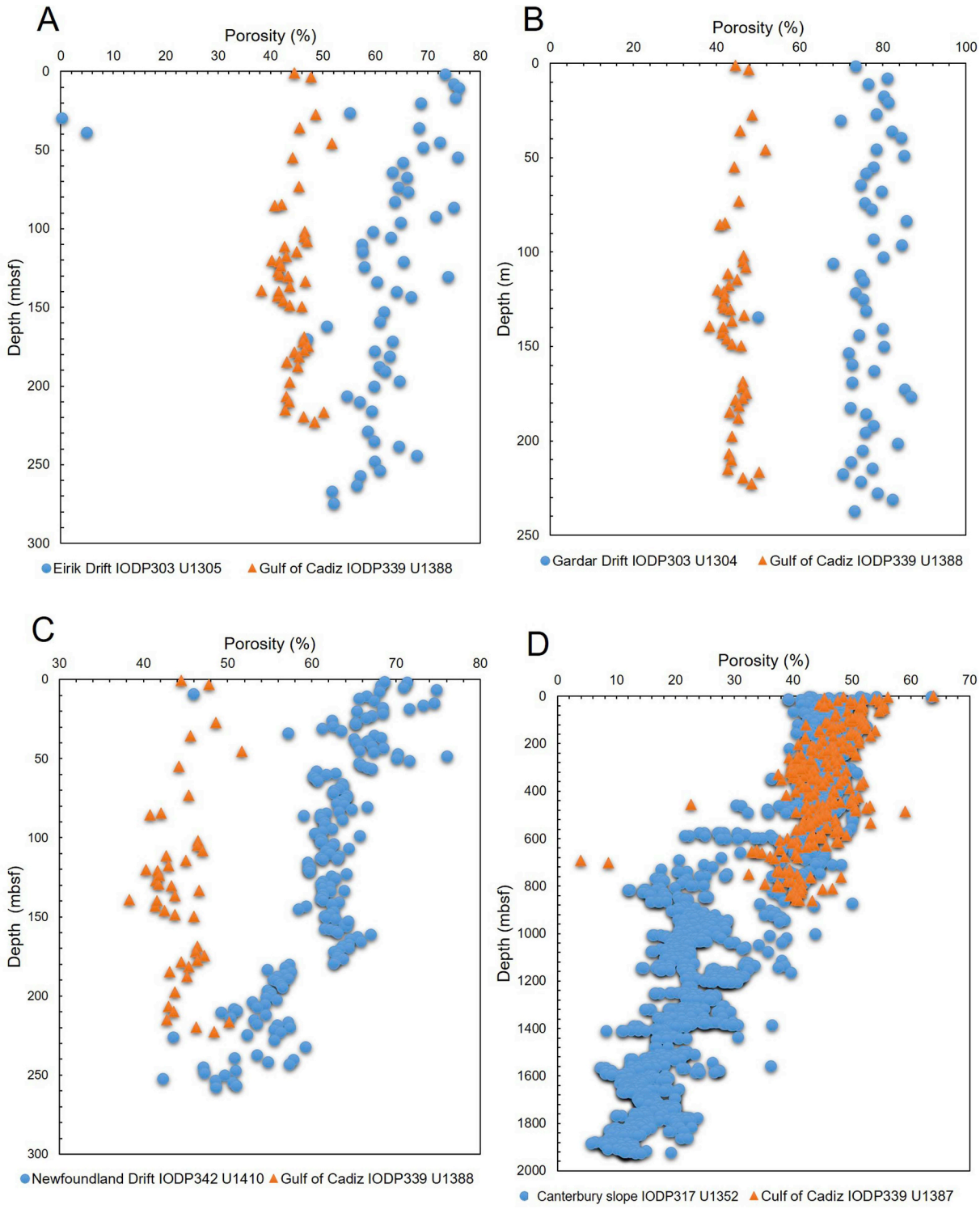

Fig. 10. Comparison of porosity-depth relationship between (A) U1305 (Eirik drift) and U1388 (Gulf of Cadiz); (B) U1304 (Gardar drift) and U1388 (Gulf of Cadiz); (C) U1410 (Newfoundland drift) and U1388 (Gulf of Cadiz); and (D) U1352 (Canterbury slope) and U1387 (Gulf of Cadiz).

porosity of around 14% for sandy contourites and 20% for muddy contourites (as predicted at 2500 m burial depth), permeabilities would be 100–1000 mD for sands and 30–150 mD for muds. These are respectable values for conventional and unconventional reservoirs, respectively.

4.4.2. *Subsurface reservoirs*

Contourite reservoirs are beginning to be recognised in the subsurface, especially those interpreted as bottom-current reworked turbidites. These include the upper parts of the giant Marlim oilfield in the Campos Basin (Moraes et al., 2007; Mutti and Carminatti, 2012), the Mzia and Coral super-giant gas fields off Mozambique (Fonnesu et al., 2020; Intawong et al., 2019; Palermo et al., 2014; Sansom, 2018), the Yinggehai basin and Baiyun sag in the northern South China Sea (Gong et al., 2016; Huang et al., 2017), and the Snorre field on the Norwegian slope (Rundberg and Eidvin, 2016). In the case of the

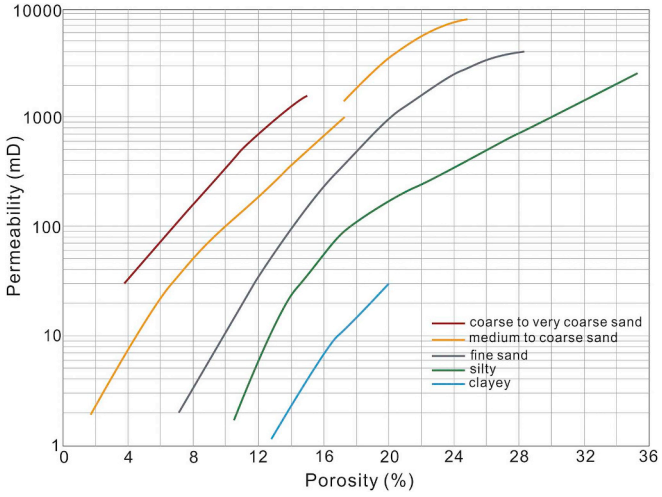

Fig. 11. Typical relationships among permeability, porosity and grain-size, modified from Chilingar (1964). Different colour lines are for different grain-size of sediments. According to Chilingar (1964), coarse to very coarse sand contains more than 50% of 0 ~ −1 phi fraction, medium to coarse sand contains more than 50% of 2–1 phi fraction, fine sand contains more than 50% of 3–2 phi fraction, silty (sandstone) contains more than 10% of silt fraction, and clayey (sandstone) contains more than 7% of clay fraction. (For interpretation of the references to colour in this figure legend, the reader is referred to the Web version of this article.)

Marlim field, the reworked facies are interpreted as highly bioturbated fine to medium contourite sands, relatively more poorly sorted than the associated turbidite sands with a muddy matrix. The porosity is typically 20–30% and the permeability around tens of millidarcies, although some mud-rich intervals with very low permeability form baffles or barriers. However, according to Moraes et al. (2007), the contourites have good lateral continuity, and even those contourites with bioturbation and cement still form good quality reservoir.

In the Santos basin, offshore Brazil, Mutti et al. (2014) interpret both bottom-current reworked turbidite reservoirs and sandy contourite reservoirs with little evidence of downslope supply, although Viana (2008) also notes the existence of coarse-grained turbidites as the likely source of extensive redistribution by bottom currents. Seismic attribute mapping from 3D seismic show a number of morphological features attributed to bottom currents, including large abyssal sand dunes, barchan dunes, sand ribbons, sand waves and furrows, all with an along-slope orientation. These sandy contourites are mainly fine sands, well sorted with low clay matrix, and show good primary porosity (over 35% in places) and high permeability. They are laterally extensive and up to hundreds of meters in thickness.

In the study of Bein and Weiler (1976), parts of the Cretaceous Talme Yafe Formation are described as including carbonate-rich contourites deposited on a continental slope. This formation is over 3 km thick and covers a large area of the Arabian Craton in Israel. The sediments are mainly dominated by very fine to very coarse-grained siliciclastics, but also include significant biochemical carbonate and carbonate skeletal fragments. Deposition is interpreted as due to both gravity currents and bottom currents. Some of the coarser sediments are believed to have been supplied by bottom-currents generated by storms. The Helez-Brur-Kokhaw oil field is reservoired in the Talme Yafe Formation, with some of the production coming from carbonate and mixed bioclastic-siliciclastic contourites (Bein and Sofer, 1987).

Unconventional reservoirs are now a hugely important and growing source of oil and gas exploration and production worldwide. Generally, these reservoirs consist of fine-grained sediment (mud and silt), have very low to low porosity values (below 10%), low to very low permeability (below 20 mD), and high total organic carbon content (normally over 2 wt%) (Zhu et al., 2012; Benayad et al., 2013; Bruna et al., 2013; Haris et al., 2017; Mahmood et al., 2018; Yang, 2018). Some authors have suggested that the highly productive shale-gas reservoirs of the Interior Seaway in the USA may be contourites in part (Viana, 2008). A similar interpretation has recently been proposed for the Ordovician-Silurian Longmaxi shale-gas formation in China (Li et al., 2016). We have reservations about both these interpretations, but further work is required.

However, the data presented in this study does suggest that fine-grained contourites have many of the characteristics that would make them good unconventional reservoirs. The interbedding of more silt-rich and mud-rich layers, the porosity-depth profiles, anomalies and over-pressured zones, as well as their great thickness and lateral extent are all favourable attributes. We are currently studying the total organic carbon (TOC) content and type for contourite systems globally, and preliminary results show many with high values (> 2% TOC). Shipboard data from the Cadiz contourites show 1–2% TOC for most of the muddy contourites, increasing to 4% for some of the interbedded contourite-turbidite section (Stow et al., 2013a).

5. Conclusions

This study presents new grain-size data for contourites from the Gulf of Cadiz, which has led to improved understanding of the contourite depositional process and primary information for reservoir characterisation in the subsurface. Furthermore, it presents contourite porosity data for the first time from four Cadiz sites and from four other IODP contourite sites, for comparison. Porosity-depth profiles, and exponential models for porosity prediction at reservoir depths, are considered in the light of growing interest in the hydrocarbon prospectivity of contourites. The key findings of significance are:

- Contourite facies can be considered according to their principal grain-size properties. We recognise three main types, as follows.
- Clay to fine silt contourites (2–20 μm) show normal grain-size distributions, poor to very poor sorting becoming better with decreasing grain size, and zero or low skewness. These are deposited by settling from weak bottom currents with a very fine suspension load and by hemipelagic settling – they are contourite-hemipelagite hybrids. Flocculation of the finest material is of key importance.
- Medium silt to fine-grained sandy contourites (20–200 μm) show a distinctive contourite depositional trend towards better sorting and coarse-tail skew. The weaker currents deposit material directly from suspended load (limited by current capacity), and then, as current velocity increases, more of the finest fraction remains in suspension, and increased winnowing and saltation becomes more important.
- Medium to coarse sandy contourites (200–1200 μm) show a trend towards poorer sorting. They result from the action of dominant bedload transport, extensive winnowing, and only intermittent bedload movement of the coarsest fraction at high current speeds.
- The nature of sediment supply to the bottom current (pelagic, hemipelagic, bottom-current erosion, shelf-slope spillover and downslope turbidity currents) is of key importance for all contourite facies.
- Porosity-depth relationships from the four Cadiz sites show a relatively high initial porosity for both sand and mud facies (50–60%), although these values are lower than 'normal' deep-water muds and sands, perhaps due to the persistent bottom current activity.
- Porosity shows a decrease with depth to around 35–40% near 500 m burial depth. According to the exponential models of porosity with depth, contourite porosity should be10–17% for sands and 18–24% for muds at 2500 m burial depth.
- Similar porosity-depth trends are present in the Eirik, Newfoundland, Gardar and Canterbury Slope drifts, although the surface sediments show 10–20% higher primary porosity where the contourites are dominantly bioclastic in composition.
- All sites reveal anomalies and breaks in the porosity-depth trends,

linked to the interbedding of sandy and muddy facies, compositional variation (carbonate vs siliciclastic), and the presence of widespread hiatuses in the sediment record. Over-pressure and higher than normal porosities are common. Differential cementation begins below a few hundred metres burial depth.

- These results give good insight into the likely reservoir characteristics of contourites, for both conventional and unconventional reservoirs. They are comparable with those of existing contourite fields, although most of these are mixed turbidite-contourite systems. We now need a deliberate search for the contourite play in the subsurface.

Acknowledgements

Many people are to thank for the collection and release of the data used in this study. In particular, we thank the captain, officers and crew, and the scientific and technical shipboard parties of the different IODP expeditions utilised. We each thank our respective institutes for their ongoing support. Xiaohang Yu acknowledges financial support from the National Natural Science Foundation of China (No. 41976067).

Appendix A. Supplementary data

Supplementary data to this article can be found online at https://doi.org/10.1016/j.marpetgeo.2020.104392.

References

Allison, E., Ledbetter, M.T., 1982. Timing of bottom-water scour recorded by sedimentological parameters in the South Australian Basin. Mar. Geol. 46, 131–147.
Alonso, B., Ercilla, G., Casas, D., Stow, D.A.V., Rodríguez-Tovar, F.J., Dorador, J., Hernández-Molina, F.-J., 2016. Contourite vs gravity-flow deposits of the pleistocene faro drift (gulf of Cadiz): sedimentological and mineralogical approaches. Mar. Geol. 377, 77–94.
Athy, L.F., 1930. Density, porosity and compaction of sedimentary rocks. AAPG (Am. Assoc. Pet. Geol.) Bull. 14, 1–24.
ASTM International, 1990. Standard method for laboratory determination of water (moisture) content of soil and rock (Standard D2216–90). In: Annual Book of ASTM Standards for Soil and Rock Am. Soc. Testing Mater., Philadelphia 04.08.
Bein, A., Sofer, Z., 1987. Origin of oils in Helez region, Israel–implications for exploration in the eastern Mediterranean. AAPG (Am. Assoc. Pet. Geol.) Bull. 71, 65–75.
Bein, A., Weiler, Y., 1976. The Cretaceous Talme Yafe Formation: a contour current shaped sedimentary prism of calcareous detritus at the continental margin of the Arabian Craton. Sedimentology 23, 511–532.
Benayad, S., Park, Y.-S., Chaouchi, R., Kherfi, N., 2013. Unconventional resources in Algeria: appraisal result from the Hamra Quartzite reservoir. Geosci. J. 17, 313–327.
Blatt, H., 1992. Sedimentary Petrology, second ed. (New York).
Blott, S.J., Pye, K., 2001. GRADISTAT: a grain size distribution and statistics package for the analysis of unconsolidated sediments. Earth Surf. Process. Landforms 26, 1237–1248.
Boggs, S., 2009. Petrology of Sedimentary Rocks, second ed. (New York).
Brackenridge, R.E., Stow, D.A.V., Hernández-Molina, F.J., Jones, C., Mena, A., Alejo, I., Ducassou, E., Llave, E., Ercilla, G., A Nombela, M., 2018. Textural characteristics and facies of sand-rich contourite depositional systems. Sedimentology 65, 2223–2252.
Bridge, J., Demicco, R., 2008. Earth Surface Processes, Landforms and Sediment Deposits. Cambridge University Press.
Bruna, P.-O., Guglielmi, Y., Lamarche, J., Floquet, M., Fournier, F., Sizun, J.-P., Gallois, A., Marié, L., Bertrand, C., Hollender, F., 2013. Porosity gain and loss in unconventional reservoirs: example of rock typing in Lower Cretaceous hemipelagic limestones, SE France (Provence). Mar. Petrol. Geol. 48, 186–205.
Brunner, C.A., 1984. Evidence for increased volume transport of the Florida current in the Pliocene and pleistocene. Mar. Geol. 54, 223–235.
Buitrago, J., García, C., Cajebread-Brow, J., Jiménez, A., Martínez del Olmo, W., 2001. Contouritas: un excelente almacén casi desconocido (Golfo de Cádiz, SO de España). 1er Congreso Técnico Exploración y producción REPSOL-YPF, Madrid, pp. 24–27 2001.
Busch, W., 1989. Patterns of sediment compaction at Ocean Drilling Program sites 645, 646, and 647, Baffin Bay and Labrador sea. In: Proceedings of the Ocean Drilling Program, Scientific Results, ODP, Leg 105, Baffin Bay and Labrador Sea, pp. 781–790.
Capella, W., Hernández-Molina, F.J., Flecker, R., Hilgen, F.J., Hssain, M., Kouwenhoven, T.J., van Oorschot, M., Sierro, F.J., Stow, D.A.V., Trabucho-Alexandre, J., Tulbure, M.A., de Weger, W., Yousfi, M.Z., Krijgsman, W., 2017. Sandy contourite drift in the late Miocene Rifian Corridor (Morocco): reconstruction of depositional environments in a foreland-basin seaway. Sediment. Geol. 355, 31–57.
Channell, J.E.T., Kanamatsu, T., Sato, T., Stein, R., Alvarez Zarikian, C.A., Malone, M.J., 2006. & the expedition 339 scientists. In: Proceedings of the Integrated Ocean Drilling Program. 303/306 Integrated Ocean Drilling Program Management International, Inc., College Station TX.
Chen, H., Xie, X., Van Rooij, D., Vandorpe, T., Su, M., Wang, D., 2014. Depositional characteristics and processes of alongslope currents related to a seamount on the northwestern margin of the Northwest Sub-Basin, South China Sea. Mar. Geol. 355, 36–53.
Chilingar, G.V., 1964. Relationship between porosity, permeability, and grain-size distribution of sands and sandstones. Dev. Sedimentol. 1, 71–75.
Cooper, M.C., 1998. The use of digital image analysis in the study of laminated sediments. J. Paleolimnol. 19, 33–40.
Faugères, J.-C., Mulder, T., 2011. Contour currents and contourite drifts. In: HüNeke, H., Mulder, T. (Eds.), Developments in Sedimentology. Elsevier.
Faugères, J.-C., Stow, D.A.V., 1993. Bottom-current-controlled sedimentation: a synthesis of the contourite problem. Sediment. Geol. 82, 287–297.
Folk, R.L., Robles, R., 1964. Carbonate sands of isla perez, alacran reef complex, Yucatan. J. Geol. 72, 255–292.
Folk, R.L., Ward, W.C., 1957. Brazos River bar [Texas]; a study in the significance of grain size parameters. J. Sediment. Res. 27, 3–26.
Fonnesu, M., Palermo, D., Galbiati, M., Marchesini, M., Bonamini, E., Bendias, D., 2020. A new world-class deep-water play-type, deposited by the syndepositional interaction of turbidity flows and bottom currents: the giant Eocene Coral Field in northern Mozambique. Mar. Petrol. Geol. 111, 179–201.
Friedman, G.M., Sanders, J.E., Kopaska-Merkel, D.C., 1992. Principles of Sedimentary Deposits: Stratigraphy and Sedimentology. Macmillan College.
Fulthorpe, C.S., Hoyanagi, K., Blum, P., 2011. & the expedition 317 scientists. In: Proceedings of the Integrated Ocean Drilling Program, vol. 317 Integrated Ocean Drilling Program Management International, Inc., Tokyo.
Gluyas, J., Swarbrick, R., 2004. Petroleum Geoscience. Blackweel Science Ltd, Oxford.
Gong, C., Wang, Y., Zheng, R., Hernández-Molina, F.J., Li, Y., Stow, D.A.V., Xu, Q., Brackenridge, R.E., 2016. Middle Miocene reworked turbidites in the Baiyun sag of the pearl river mouth basin, northern South China sea margin: processes, genesis, and implications. J. Asian Earth Sci. 128, 116–129.
Gonthier, E.G., Faugères, J.-C., Stow, D.A.V., 1984. Contourite Facies of the Faro Drift, Gulf of Cadiz. vol. 15. Geological Society, London, Special Publications, pp. 275–292.
Haris, A., Seno, B., Riyanto, A., Bachtiar, A., 2017. Integrated approach for characterizing unconventional reservoir shale hydrocarbon: case study of North sumatra basin. In: IOP Conference Series: Earth Environmental Science. vol. 62. pp. 12–23.
Hernandez-Molina, F.J., Llave, E., Preu, B., Ercilla, G., Fontan, A., Bruno, M., Serra, N., Gomiz, J.J., Brackenridge, R.E., Sierro, F.J., 2014. Contourite processes associated with the mediterranean Outflow water after its exit from the strait of Gibraltar: global and conceptual implications. Geology 42, 227–230.
Hernández-Molina, F.J., Sierro, F.J., Llave, E., Roque, C., Stow, D.A.V., Williams, T., Lofi, J., Van der Schee, M., Arnáiz, A., Ledesma, S., Rosales, C., Rodríguez-Tovar, F.J., Pardo-Igúzquiza, E., Brackenridge, R.E., 2016a. Evolution of the gulf of Cadiz margin and southwest Portugal contourite depositional system: tectonic, sedimentary and paleoceanographic implications from IODP expedition 339. Mar. Geol. 377, 7–39.
Hernández-Molina, F.J., Wåhlin, A., Bruno, M., Ercilla, G., Llave, E., Serra, N., Rosón, G., Puig, P., Rebesco, M., Van Rooij, D., Roque, D., González-Pola, C., Sánchez, F., Gómez, M., Preu, B., Schwenk, T., Hanebuth, T.J.J., Sánchez Leal, R.F., García-Lafuente, J., Brackenridge, R.E., Juan, C., Stow, D.A.V., Sánchez-González, J.M., 2016b. Oceanographic processes and morphosedimentary products along the Iberian margins: a new multidisciplinary approach. Mar. Geol. 378, 127–156.
Hollister, C.D., Heezen, B.C., 1972. Geologic Effects of Ocean Bottom Currents: Western North Atlantic. Gordon and Breach Science Publications, New York.
Huang, Y., Yao, G., Zhou, F., Wang, T., 2017. Impact factors on reservoir quality of clastic Huangliu formation in overpressure diapir zone, Yinggehai Basin, China. J. Petrol. Sci. Eng. 154, 322–336.
Intawong, A., Hodgson, N., Rodriguez, K., Hargreaves, P., 2019. Oil prospects in the Mozambique Channel: where incipient subduction meets passive margin. First Break 37, 75–81.
Jansa, L.F., Urrea, V.H.N., 1990. Geology and diagenetic history of overpressured sandstone reservoirs, venture gas field, offshore Nova Scotia, Canada (1). AAPG (Am. Assoc. Pet. Geol.) Bull. 74, 1640–1658.
Ledbetter, M.T., Ellwood, B.B., 1980. Spatial and temporal changes in bottom-water velocity and direction from analysis of particle size and alignment in deep-sea sediment. Mar. Geol. 38, 245–261.
Leeder, M.R., 1999. Sedimentology and Sedimentary Basins: from Turbulence to Tectonics. Blackwell, Oxford.
Li, Y., Wang, X., Wu, B., Li, G., Wang, D., 2016. Sedimentary facies of marine shale gas formations in southern China: the lower silurian Longmaxi formation in the southern sichuan basin. J. Earth Sci. 27, 807–822.
Lüdmann, T., Betzler, C., Eberli, G.P., Reolid, J., Reijmer, J.J., Sloss, C.R., Bialik, O.M., Alvarez-Zarikian, C.A., Alonso-García, M., Blättler, C.L., 2018. Carbonate delta drift: a new sediment drift type. Mar. Geol. 401, 98–111.
Lüdmann, T., Kalvelage, C., Betzler, C., Fürstenau, J., Hübscher, C., 2013. The Maldives, a giant isolated carbonate platform dominated by bottom currents. Mar. Petrol. Geol. 43, 326–340.
Mahmood, M.F., Ahmad, Z., Ehsan, M., 2018. Total organic carbon content and total porosity estimation in unconventional resource play using integrated approach through seismic inversion and well logs analysis within the Talhar Shale, Pakistan. J. Nat. Gas Sci. Eng. 52, 13–24.
Maldonado, A., Somoza, L.s., Pallarés, L., 1999. The betic orogen and the Iberian–African boundary in the gulf of Cadiz: geological evolution (central North Atlantic). Mar. Geol. 155, 9–43.
Martins, L.R., 1965. Significance of skewness and kurtosis in environmental

interpretation. J. Sediment. Res. 35, 768–770.
Martins, L.R., 2003. Recent sediments and grain-size analysis. Gravel 1, 90–105.
Mason, C.C., Folk, R.L., 1958. Differentiation of beach, dune, and Aeolian flat environments by size analysis, Mustang Island, Texas. J. Sediment. Res. 28, 211–226.
Masson, D.G., Plets, R.M.K., Huvenne, V.A.I., Wynn, R.B., Bett, B.J., 2010. Sedimentology and depositional history of Holocene sandy contourites on the lower slope of the Faroe–Shetland Channel, northwest of the UK. Mar. Geol. 268, 85–96.
McCave, I., 1984. Erosion, Transport and Deposition of Fine-Grained Marine Sediments, vol. 15. Geological Society, London, Special Publications, pp. 35–69.
McCave, I., 2008. Size sorting during transport and deposition of fine sediments: sortable silt and flow speed. Dev. Sedimentol. 60, 121–142.
McCave, I., Bryant, R., Cook, H., Coughanowr, C., 1986. Evaluation of a laser-diffraction-size analyzer for use with natural sediments. J. Sediment. Res. 56.
McCave, I.N., Manighetti, B., Robinson, S.G., 1995. Sortable silt and fine sediment size/composition slicing: parameters for palaeocurrent speed and palaeoceanography. Paleoceanography 10, 593–610.
Moraes, M.A.S., Maciel, W.B., Braga, M.S.S., Viana, A.R., 2007. Bottom-current Reworked Palaeocene-Eocene Deep-Water Reservoirs of the Campos Basin. Geological Society of London, *Brazil,* London.
Mulder, T., Hassan, R., Ducassou, E., Zaragosi, S., Gonthier, E., Hanquiez, V., Marchès, E., Toucanne, S., 2013. Contourites in the Gulf of Cadiz: a cautionary note on potentially ambiguous indicators of bottom current velocity. Geo Mar. Lett. 33, 357–367.
Mutti, E., Carminatti, M., 2012. Deep-water Sands of the Brazilian Offshore Basins. Search Discovery.
Mutti, E., Cunha, R.S., Bulhoes, É.M., Arienti, L.M., 2014. Contourites and Turbidites of the Brazilian Marginal Basins. AAPG Annual Convention & Exhibition, Houston, USA.
Nicholson, U., Stow, D., 2019. Erosion and deposition beneath the subantarctic front since the early Oligocene. Sci. Rep. 9, 9296.
Norris, R.D., Wilson, P.A., Blum, P., 2014. & the expedition 339 scientists. In: Proceedings of the Integrated Ocean Drilling Program, vol. 342 Integrated Ocean Drilling Program Management International, Inc., College Station TX.
Osborne, M., Swarbrick, R., 1997. Mechanisms for generating overpressure in sedimentary basins_ A reevaluation. AAPG (Am. Assoc. Pet. Geol.) Bull. 81, 1032–1041 1997.
Palermo, D., Galbiati, M., Famiglietti, M., Marchesini, M., Mezzapesa, D., Fonnesu, F., 2014. In: Insights into a New Super-giant Gas Field-Sedimentology and Reservoir Modeling of the Coral Reservoir Complex, Offshore Northern Mozambique. Offshore Technology Conference-Asia (Offshore Technology Conference).
Pettingill, H.S., Weimer, P., 2002. Worlwide deepwater exploration and production: past, present, and future. Lead. Edge 21, 371–376.
Pollack, J.M., 1961. Significance of compositional and textural properties of south Canadian river channel sands, New Mexico, Texas and Oklahoma. J. Sediment. Res. 31, 795–801.
Rebesco, M., Camerlenghi, A., 2008. Contourites. Elsevier Science, Amsterdam.
Rebesco, M., Hernández-Molina, F.J., Van Rooij, D., Wåhlin, A., 2014. Contourites and associated sediments controlled by deep-water circulation processes: state-of-the-art and future considerations. Mar. Geol. 352, 111–154.
Rubey, W.W., Hubbert, M.K., 1959. In: Role of Fluid Pressure in Mechanics of Overthrust Faulting. vol. 70 Geological Society of America Bulletin.
Rundberg, Y., Eidvin, T., 2016. Discussion on 'late cenozoic geological evolution of the northern North Sea: development of a Miocene unconformity reshaped by large-scale pleistocene sand intrusion' journal of the geological society, 170, 133–145. J. Geol. Soc. 173, 384–393.
Sansom, P., 2018. Hybrid turbidite–contourite systems of the Tanzanian margin. Petrol. Geosci. 24, 258–276.
Scherer, M., 1987. Parameters influencing porosity in sandstones: a model for sandstone porosity prediction. AAPG Bull. 71, 485–491.
Sclater, J.G., Christie, P.A.F., 1980. Continental stretching: an explanation of the post-mid-cretaceous subsidence of the central North Sea basin. J. Geophys. Res.: Solid Earth 85, 3711–3739.
Selley, R.C., 2000. Applied Sedimentology. Elsevier.
Shanmugam, G., 2006. Deep-water Processes and Facies Models: Implications for Sandstone Petroleum Reservoirs. Elsevier.
Shanmugam, G., 2012. New Perspectives on Deep-Water Sandstones: Origin, Recognition, Initiation, and Reservoir Quality, vol. 9 Elsevier.
Shanmugam, G., 2017. Contourites: physical oceanography, process sedimentology, and petroleum geology. Petrol. Explor. Dev. 44, 183–216.
Stow, D.A.V., 2005. Sedimentary Rocks in the Field: A Colour Guide. CRC Press.
Stow, D.A.V., Armishaw, J.E., Holmes, R., 2002a. Holocene Contourite Sand Sheet on the Barra Fan Slope, NW Hebridean Margin. vol. 22. Geological Society, London, Memoirs, pp. 99–119.
Stow, D.A.V., Brackenridge, R., Hernandez-Molina, F.J., 2011. Contourite Sheet Sands: New Deepwater Exploration Target. American Association of Petroleum Geologists Annual Conference, Houston.
Stow, D.A.V., Faugères, J.-C., Howe, J.A., Pudsey, C.J., Viana, A.R., 2002b. Bottom currents, contourites and deep-sea sediment drifts: current state-of-the-art. 22. Geological Society, London, Memoirs, pp. 7–20.
Stow, D.A.V., Faugères, J.C., 2008. Contourite facies and the facies model. In: Rebesco, M., Camerlenghi, A. (Eds.), Developments in Sedimentology. Elsevier.
Stow, D.A.V., Hernández-Molina, F., Zarikian, C., Expedition Shipboard Scientists, 2014. New Advances in the Contourite Paradigm: IODP Expedition 339. Gulf of Cadiz. 2nd Deep-Water Circulation Congress. Ghent, Belgium.
Stow, D.A.V., Hernández-Molina, F.J., Alvarez Zarikian, C.A., 2013a. Expedition 339 scientists. In: Proceedings of the Integrated Ocean Drilling Program, vol. 339 Integrated Ocean Drilling Program Management International, Inc., Tokyo.
Stow, D.A.V., Hernández-Molina, F.J., Llave, E., Bruno, M., García, M., Díaz del Rio, V., Somoza, L., Brackenridge, R.E., 2013b. The Cadiz Contourite Channel: sandy contourites, bedforms and dynamic current interaction. Mar. Geol. 343, 99–114.
Stow, D.A.V., Holbrook, J.A., 1984. North Atlantic contourites: an overview. Geol. Soc., Lond., Spec. Publ. 15 (1), 245–256.
Stow, D.A.V., Hunter, S., Wilkinson, D., Hernández-Molina, F.J., 2008. The nature of contourite deposition. In: Rebesco, M., Camerlenghi, A. (Eds.), Developments in Sedimentology.
Stow, D.A.V., Mayall, M., 2000. Deep-water sedimentary systems: new models for the 21st century. Mar. Petrol. Geol. 17, 125–135.
Stricker, S., Jones, S.J., 2018. Enhanced Porosity Preservation by Pore Fluid Overpressure and Chlorite Grain Coatings in the Triassic Skagerrak, vol. 435. Geological Society London Special Publications, Central Graben, North Sea, UK, pp. 321–341.
Viana, A.R., 2008. Economic relevance of contourites. In: Rebesco, M., Camerlenghi, A. (Eds.), Developments in Sedimentology. Elsevier.
Viana, A.R., Almeida JR., W., Nunes, M.C.V., Bulhoese, M., 2007. The Economic Importance of Contourites. Geological Society of London, London.
Viana, A.R., Faugeres, J.C., Stow, D.A.V., 1998. Bottom-current-controlled sand deposits - a review of modern shallow- to deep-water environments. Sediment. Geol. 115, 53–80.
Wangen, M., 2010. Generation of overpressure by cementation of pore space in sedimentary rocks. Geophys. J. Int. 143, 608–620.
Waples, D.W., Couples, G.D., 1998. Some Thoughts on Porosity Reduction – Rock Mechanics, Overpressure and Fluid Flow, vol. 141. Geological Society London Special Publications, pp. 73–81.
Wen, Z., Xu, H., Wang, Z., He, Z., Song, C., Chen, X., Wang, Y., 2016. Classification and hydrocarbon distribution of passive continental margin basins. Petrol. Explor. Dev. 43, 740–750.
Wentworth, C.K., 1922. A scale of grade and class terms for clastic sediments. J. Geol. 30, 377–392.
Yang, B., 2018. Geological characteristics and reservoir properties in the unconventional Montney Formation, southwestern Alberta, Canada. Geosci. J. 22, 313–325.
Zhu, G., Gu, L., Su, J., Dai, J., Ding, W., Zhang, J., Song, L., 2012. Sedimentary association of alternated mudstones and tight sandstones in China's oil and gas bearing basins and its natural gas accumulation. J. Asian Earth Sci. 50, 88–104.